International
Progress Report

IPR-10-07

Äspö Hard Rock Laboratory

Äspö Task Force on Engineered Barrier System

Modelling of THM-coupled processes for benchmark 2.2 with the code GeoSys/RockFlow

Thomas Nowak
Herbert Kunz

Federal Institute for Geosciences
and Natural Resources, Hannover, Germany

February 2010

Svensk Kärnbränslehantering AB
Swedish Nuclear Fuel
and Waste Management Co

Box 250, SE-101 24 Stockholm
Phone +46 8 459 84 00

Äspö Hard Rock
Laboratory

Report no.
IPR-10-07
No.
F89K
Author
Thomas Nowak
Herbert Kunz
Date
February 2010
Checked by
Anders Sjöland
Date
2010-06-08
Approved
Mats Ohlsson
Date
2010-06-11

Äspö Hard Rock Laboratory

Äspö Task Force on Engineered Barrier System

Modelling of THM-coupled processes for benchmark 2.2 with the code GeoSys/RockFlow

Thomas Nowak
Herbert Kunz

Federal Institute for Geosciences
and Natural Resources, Hannover, Germany

February 2010

Keywords: Task Force, Engineered Barrier System, Modelling, Bentonite, Buffer, Thermal, Hydraulic, Mechanical

Abstract

In 2004 the Swedish Nuclear Fuel and Waste Management Co. (SKB) initiated the project “Task Force on Engineered Barrier Systems”. This project has the objective to verify the feasibility of modelling THM-coupled processes (task 1) and gas migration processes (task 2) in clay-rich buffer materials. The tasks are performed on the basis of appropriate benchmarks.

This report documents the modelling results of the THM-benchmark 2.2 - the Canister Retrieval Test - using the code GeoSys/RockFlow. The Temperature Buffer Test which was performed in the immediate vicinity of the Canister Retrieval Test is included in the model. Especially the heat transport requires the handling of the problem in 3-D. Due to limitations imposed by post-processing different spatial discretisations of the model had to be used during the processing of the benchmark.

The calculated temperatures agree well with measured data. Concerning hydraulic parameters the values of permeability and tortuosity were varied in the calculations. The time necessary to saturate the buffer is very sensitive to both of these values. In comparison to thermal and hydraulic processes the model only has limited capacity to predict the measured evolution of total pressure.

Sammanfattning

2004 initierade Svensk Kärnbränslehantering AB, SKB, projektet ”Task Force on Engineered Barrier Systems”. Syftet med detta projekt är att verifiera möjligheten att modellera THM-kopplade processer (Task 1) och gasmigrationprocesser (Task 2) i lerbaserade buffertmaterial. Lämpliga laboratorie- och fältförsök ligger till grund för modelleringsuppgifterna.

Denna rapport beskriver resultaten av modelleringen av THM-kopplade processer för Task 2 (Benchmark 2.2, the Canister Retrieval Test) med hjälp av koden GeoSys/RockFlow. Temperature Buffer Test, vilket utfördes i direkt närhet till Canister Retrieval Test, inkluderas i modellen. Framförallt värmetransporten kräver behandling av problemet i 3-D. På grund av begränsningar åsamkade av efterbearbetning har man fått använda olika volymvariationer av modellen under bearbetningen av Benchmark 2.2.

De kalkylerade temperaturerna stämmer bra överens med mätdata. Beträffande hydrauliska parametrar varierades värdet för permeabilitet och mekanik under beräkningarna. Tiden för att mätta bufferten är mycket känslig för båda dessa värden. I jämförelse med termiska och hydrauliska processer har modellen enbart begränsade möjligheter att prediktera det uppmätta förloppet för totalt tryck.

Contents

1 Introduction

Modelling coupled thermal, hydraulic, mechanical, and chemical processes is of importance for the investigation of different concepts for final repositories. The radioactive waste heats the surrounding system of engineered and geological barriers, and this process shows strong interactions with hydraulic, mechanical, and chemical processes.

In many concepts for final repositories clay-rich materials play an important role as a technical barrier. Due to adsorption of water into the clay mineral lattice these materials are capable of swelling. Changes in water saturation of this technical barrier are caused on the one hand by evaporation of water due to the heat generated by the waste, on the other hand by water from the host rock infiltrating into the technical barrier. The ability to understand and model these opposing processes is of special importance for the performance of a final repository for high level waste in crystalline rock and clay.

Several in-situ experiments with clay-rich materials as buffer material were conducted in underground research laboratories in crystalline rock. The data gained by these experiments (i.e. temperature, relative humidity, total stress) put the numerical tools to the test that are going to be used for the calculation of a repository layout. BGR uses the code GeoSys/RockFlow (GS/RF) for repository layouts in crystalline rock and clay(-stone). This code proved to be suitable for modelling the behaviour of clay-rich materials (see for example SHAO & NOWAK 2008, NOWAK & KUNZ 2009).

This report describes the final results of the modelling of the Canister Retrieval Test (CRT) in the Äspö Hard Rock Laboratory (HRL) that was chosen as benchmark (BM) in the project "Task Force on Engineered Barrier Systems". Though it was beyond the scope of that benchmark, the Temperature Buffer Test (TBT) which is located centre-to-centre 6 m from the CRT was included into the model.

Na-bentonite MX-80 was used in both in-situ experiments as buffer material. Beside several laboratory experiments which were performed to investigate the basic parameters of this material, there was a laboratory experiment which had been used as BM 1.1.1 in this project (NOWAK 2007). The governing equations of the code can also be found in WANG et al. (2009) or the previously cited report.

2 Experiments

2.1 Canister Retrieval Test

The Canister Retrieval Test (CRT) was chosen as BM 2.2. The main purpose of this experiment was to demonstrate the capability of retrieving deposited nuclear waste, but it has also been used to record the THM processes in the Swedish KBS-3V deposit technique. The deposition tunnel for the experiment is located on the 420-metre level and was excavated by conventional drill and blast, see Figure 2-1. The excavations which are included in the 3-D model (compare chapter 3.1) are shaded in blue.

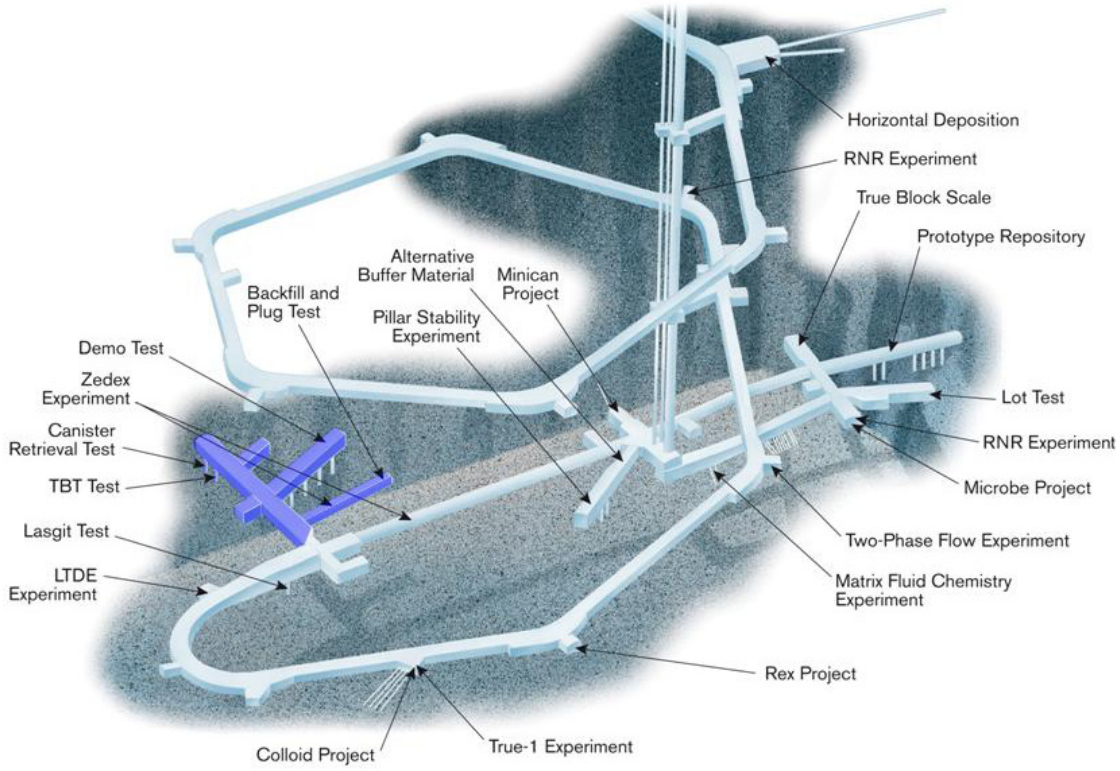

Figure 2-1. *Overview of the Äspö HRL (picture from SKB).*

The drilled deposition hole is 8.55 metres deep. Slots were cut into the wall of the deposition hole for cables to prevent them from being damaged. As the supply of water from the rock was judged to be insufficient for saturating the buffer an artificial pressurised saturation system (filter mats attached to the wall of the deposition hole) was built. The surrounding rock at the upper part of the hole mainly consists of greenstone and the lower part of Äspö diorite.

The bentonite buffer was installed mainly in form of blocks and rings of bentonite, see Figure 2-2 (dimensions are given in mm). The blocks have a diameter of 1.65 m and a height of 0.5 m. When the stack of blocks and rings was 6 m high, the canister, equipped with electrical heaters, was lowered down into the centre of the hole. Bentonite bricks were emplaced on the top of the canister and additional blocks were

emplaced until the hole was filled to a distance of one metre below the tunnel floor. The top of the hole was sealed with a retaining plug made of concrete and with a steel plate. The plug was secured against heave caused by the swelling clay with nine cables anchored in the rock. Water was supplied artificially to gain saturation around the bentonite blocks.

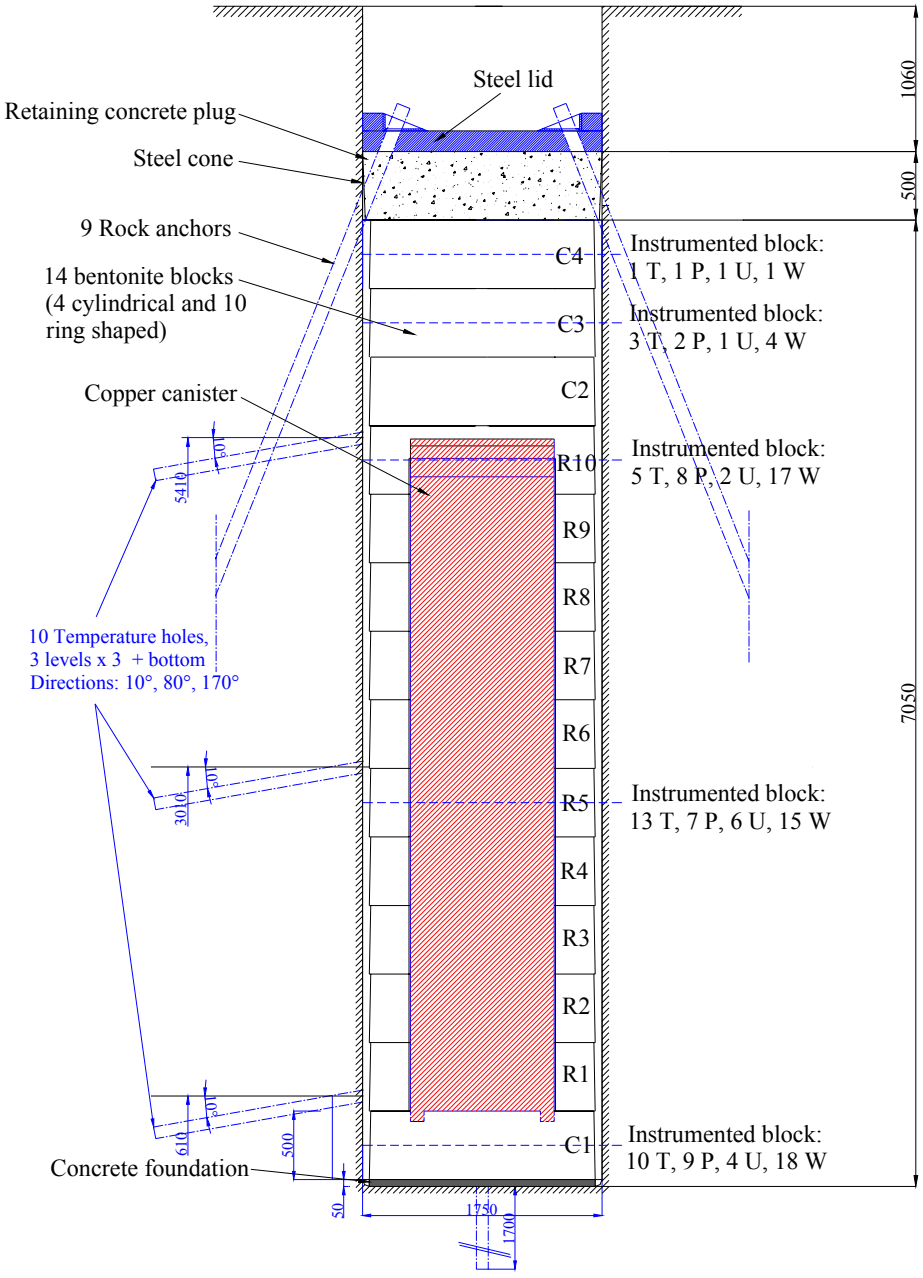

Figure 2-2. *Schematic drawing of the CRT layout (picture from SKB).*

Test installation was carried out in the following order:

- preparations on site – concrete foundation, cutting of slots in the wall of the deposition hole, drilling for rock anchors and instruments, installation of rock anchors, filter mats for saturation, installation of formwork for plug,
- emplacement of bentonite blocks and rings including the installation of instruments,
- deposition of canister,
- continuation of emplacement of bentonite bricks, blocks, and rings including installation of instruments,
- filling of void between rock and bentonite rings with bentonite pellets and water (October 26, 2000),
- casting of concrete plug and placement of steel lid,
- pre-stressing of retaining system.

When the pellet-filled outer slot was filled with water, the estimated amount of water to fill up the voids between the pellets was exceeded. The water is thought to have penetrated through the interfaces between the bentonite blocks into the inner gap between canister and rings and thereby got access to an additional volume to fill. Sensor data is also indicating that the inner slot was filled with water.

Heating was started with an initially applied constant power of 700 W one day after casting the plug. The displacements and forces on the plug were checked and monitored during the initial phase when the plug was only fixed by three anchors. When the total force exceeded 1500 kN, the remaining anchors were fixed in the required manner. This took place between 46 and 48 days after test start.

The canister heating power was raised twice: to 1700 W on November 13, 2000 and to 2600 W on February 13, 2001. The filter pressure was raised gradually starting on September 5, 2002 to a value of 0.8 MPa on October 10, 2002. For more details of the evolution of heater power and filter pressure see chapter 3.2.

2.2 Temperature Buffer Test

The French National Radioactive Waste Management Agency (ANDRA) carries out the Temperature Buffer Test (TBT) in co-operation with SKB. The experiment is intended to increase the understanding of the THM-behaviour of engineered barriers during the water saturation transient, including temperatures above 100°C (ÅKESSON 2006). The TBT has considerable thermal effects on the CRT experiment since the hole-centers are located only 6 m apart.

The experiment includes two heaters in the axis of the deposition hole which are separated by a compacted bentonite block, compare Figure 2-3 (dimensions are in mm). The heaters are 3 m long and 610 mm in diameter. Each one simulates a different confinement system: a bentonite buffer only (bottom section) and a bentonite buffer with an inner sand shield (upper section). An artificial water pressure is applied in the slot between the buffer and the rock. The slot is filled with sand (ÅKESSON 2006).

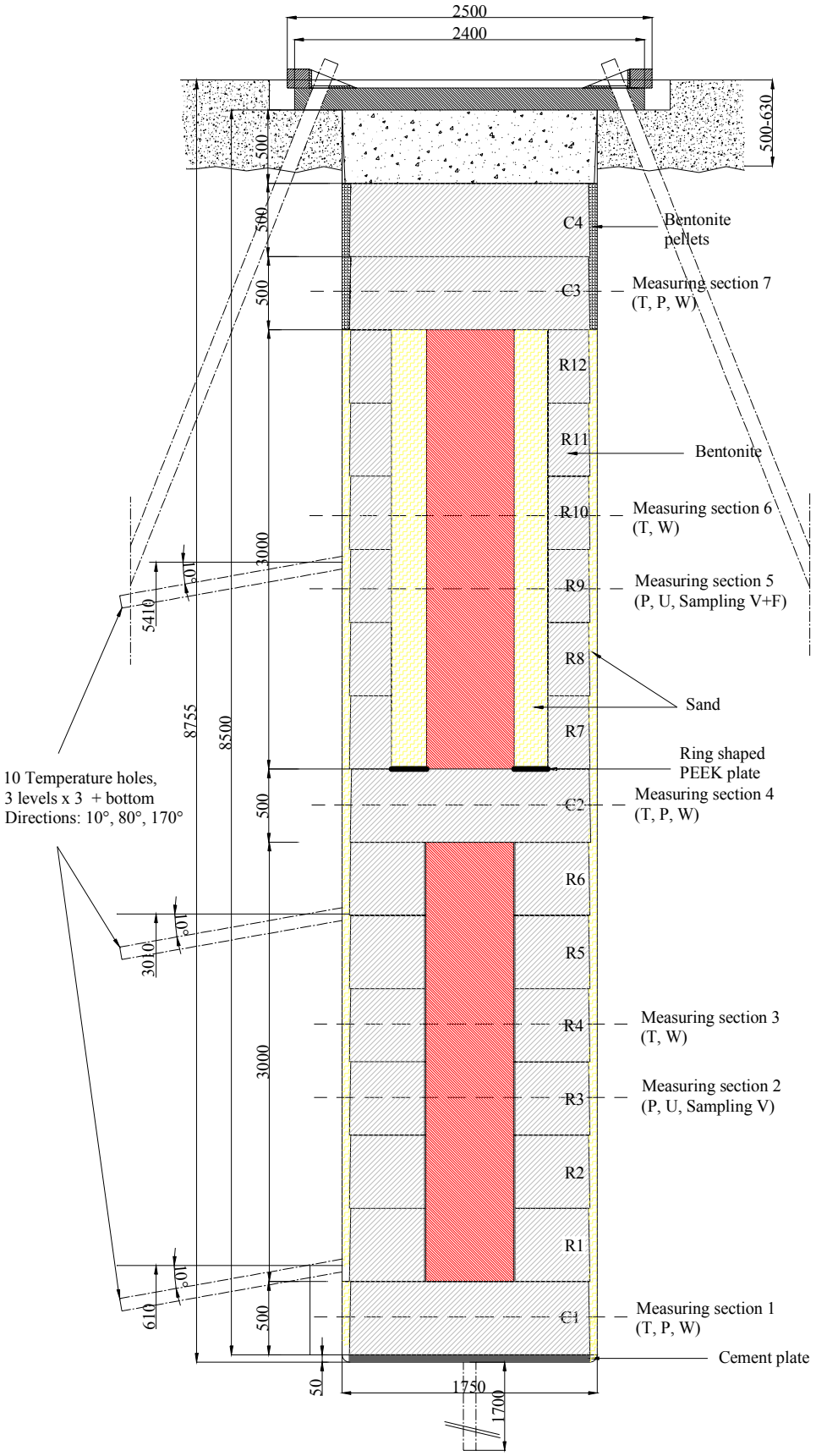

Figure 2-3. *Schematic drawing of the TBT layout (picture from SKB).*

3 Model

During the processing of this benchmark several spatial discretisations of the modelling domain had been used. THM-coupled calculations had been performed with all of these dicretisations, but finally not all of them turned out to be testable for the correct transfer of the input data into the numerical model and evaluable with the available post-processing tools. The results for total pressure and the results for temperature and water content (measured as suction or relative humidity) presented in chapter 4 had been gained with different spatial discretisations, but the boundary conditions and source terms of the model are essentially identical. In the final phase of processing this benchmark the focus had been on the influence of permeability and tortuosity on the time necessary to saturate the buffer.

The governing equations of the code can also be found in WANG et al. (2009) or in the modelling report for the benchmarks 2.1.1 and 2.1.1 (NOWAK & KUNZ 2009).

3.1 Finite Element Meshes

The geometry of the modelling domain was created as follows:

- digitalization of the ground view of the 420-metre level where the following experiments are located (compare Figure 2-1): CRT, TBT, ZEDEX, Backfill and Plug Test, Demo Test,
- extruding the digitized ground view in z-direction, modifying the width of the 420-metre level excavations for a rounded contour,
- digital construction of CRT- and TBT-geometry with the given dimensions,
- and finally adding the geometry of outer boundaries for the modelling domain.

The face towards the rest of the laboratory is located along the TBM assembly hall where the LASGIT is located (compare Figure 2-1). The upper and lower boundaries are in the xy-plane and perpendicular to these the other boundaries are aligned, each located several decametres from the open excavations.

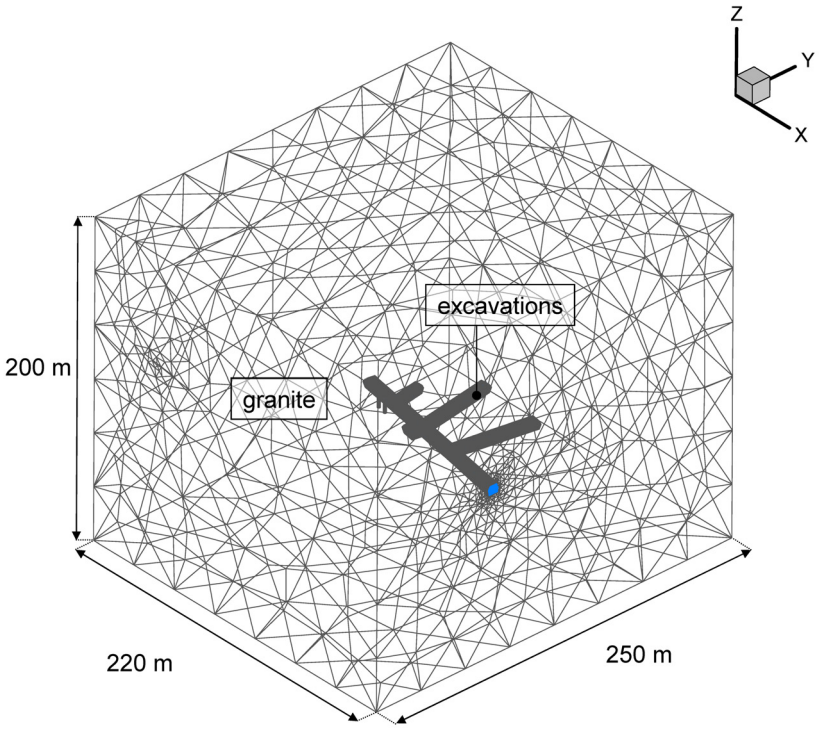

Figure 3-1. *Mesh for CRT/TBT model.*

This geometry has been discretised in space with two different meshes: one for the TH-coupled calculations and a coarser mesh for the THM-coupled calculations. Though the finer mesh works also for the THM-coupled calculations the calculation time becomes very large and especially the post-processing of the results is hardly operable with common 32-bit operating systems. The results for the total pressure presented in chapter 4.6 are from the discretisation which was presented in May 2008 at the Task Force meeting in Äspö. The main difference to the mesh for the TH-coupled calculation which is presented in detail in the following is the coarser discretisation (26017 nodes, 153748 elements). The outer layer of bentonite pellets in CRT and the sand filter in TBT are ignored in the THM-mesh, instead the different bentonite materials are in direct contact with the rock.

In the mesh for the TH-coupled calculations there are 115219 nodes in 727111 tetrahedral elements in total. For the bentonite rings, blocks, bricks, and pellets in CRT 30661 nodes (161739 elements) are used and 27193 nodes (108850 elements) for the bentonite rings and blocks and the sand in TBT. These numbers result from the geometry itself and following volume constraints:

- < 0.0003 m^3 for the bentonite blocks in CRT and TBT
- < 0.0002 m^3 for the bentonite rings in TBT
- < 0.00015 m^3 for the bentonite rings and bricks in CRT

Figure 3-2 shows the TH-mesh around CRT and TBT; the elements for the rock, the pellets in both experiments, and the sand filter in TBT are blanked in this figure and only the outer surfaces of elements are shown. The automatic decomposition for parallel processing on 8 processors results in sub-domains ranging between 88243 and 93252 elements in size.

For the THM-mesh the outer layer of bentonite pellets in CRT has not been taken into account and instead has been modelled with the elements for the bentonite rings and blocks. The sand filter in TBT has also not been taken into account and instead has been modelled with the elements for bentonite 1 and 2.

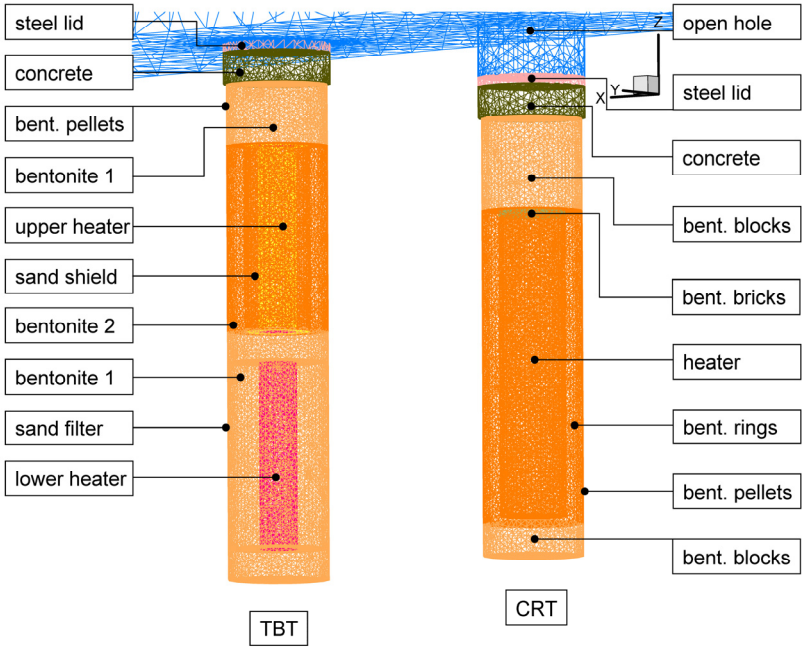

Figure 3-2. *Detail TBT (left hand side) and CRT (right hand side) of the mesh.*

3.2 Initial and Boundary Conditions and Source Terms

Initially (day -720) there is a hydrostatic pressure distribution in the entire modelling domain. The calculation starts two years before the installation of CRT in order to generate an approximated initial hydraulic state of the rock. Open excavation surfaces are put under a water pressure of 0.1 MPa (atmospheric pressure); outer boundaries are put under hydrostatic pressure. In the first year (until day -360) the 420-metre level is open, then both CRT- and TBT-borehole are open (until day 0). The complete calculation sequence is depicted in Table 3-1. The sequence was intended to create a reasonable pressure distribution in the model at CRT installation to allow for modelling the saturation via the filters with a water source term. Finally this alternative to the filter pressure boundary conditions was not used due to the time limitation of processing this benchmark exercise.

Table 3-1. Calculation sequence for CRT/TBT model.

time [d]	description (change of conditions)	steps
-720 to -360	420-metre level open except CRT- and TBT-borehole	12
-360 to 0	420-metre level open incl. CRT- and TBT-borehole	12
0 - 796	CRT in place	390
796 - 1877	CRT and TBT in place	396
1877 - 2883	CRT dismantled, TBT in place	292

The bentonite rings and blocks in CRT have a water pressure of -37 MPa (suction) at installation (day 0). For the blocks this equals a water saturation of 0.751 and for the rings this equals a water saturation of 0.849. The bentonite bricks have a water pressure of -37.5 MPa (suction) at installation. For the bricks this equals a water saturation of 0.637.

The bentonites "type 1" and "type 2" in TBT have a water pressure of -47.5 MPa (suction) at installation (day 796). For these types this equals a water saturation of 0.798 (ÅKESSON 2006).

Both experiments are saturated artificially via filters. The pressure evolution in these filters depicted in Figure 3-3 is used as boundary condition in the model. In TBT the sand filter was initially dry.

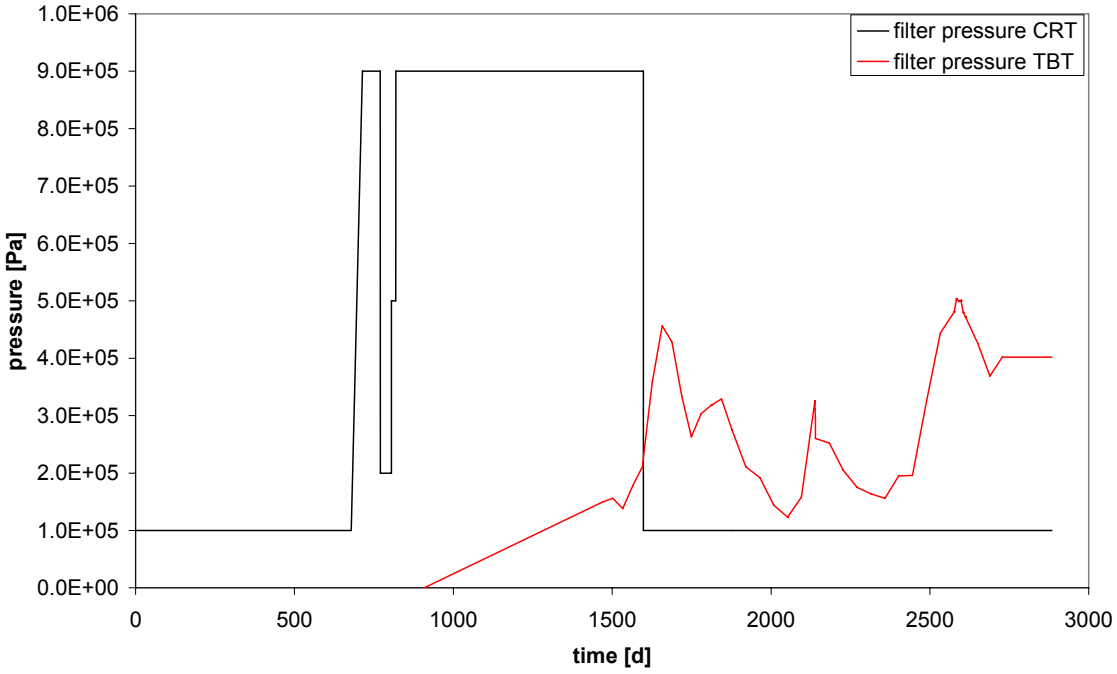

Figure 3-3. *Filter pressures in the model.*

Mechanical boundary conditions are summarized in Figure 3-4. The load on top represents the overburden pressure. The resulting stress field was not adjusted to a measured stress field.

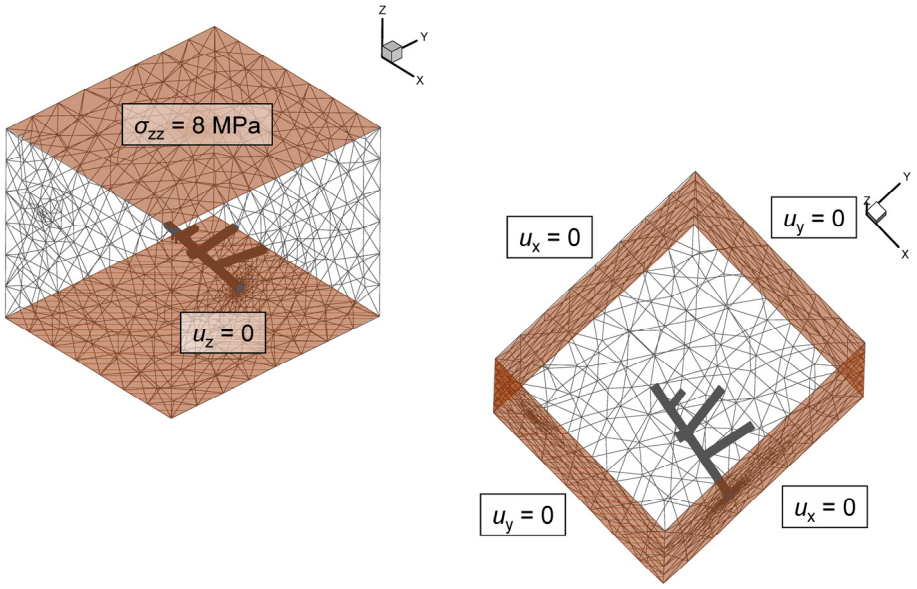

Figure 3-4. *Mechanical boundary conditions.*

Initially there is a temperature of 17°C in the entire modelling domain. Thermal boundary conditions are 17°C at all outer boundaries. The intended changes of heater power are listed in Table 3-2. The actual heat sources in the model include also malfuntions as indicated in Figure 3-5.

Table 3-2. Intended heater power steps.

time [d]	heater CRT [W]	lower heater TBT [W]	upper heater TBT [W]
0	0		
1	700		
18	1700		
110	2600		
684	2100		
881		900	900
889		1200	1200
896		1500	1500
1135	1600		
1596	1150		
1811	0		
2052		1600	1600
2579		1700	1500
2583		1800	1400
2590		1900	1300
2597		2000	1200
2604			1100
2611			1000

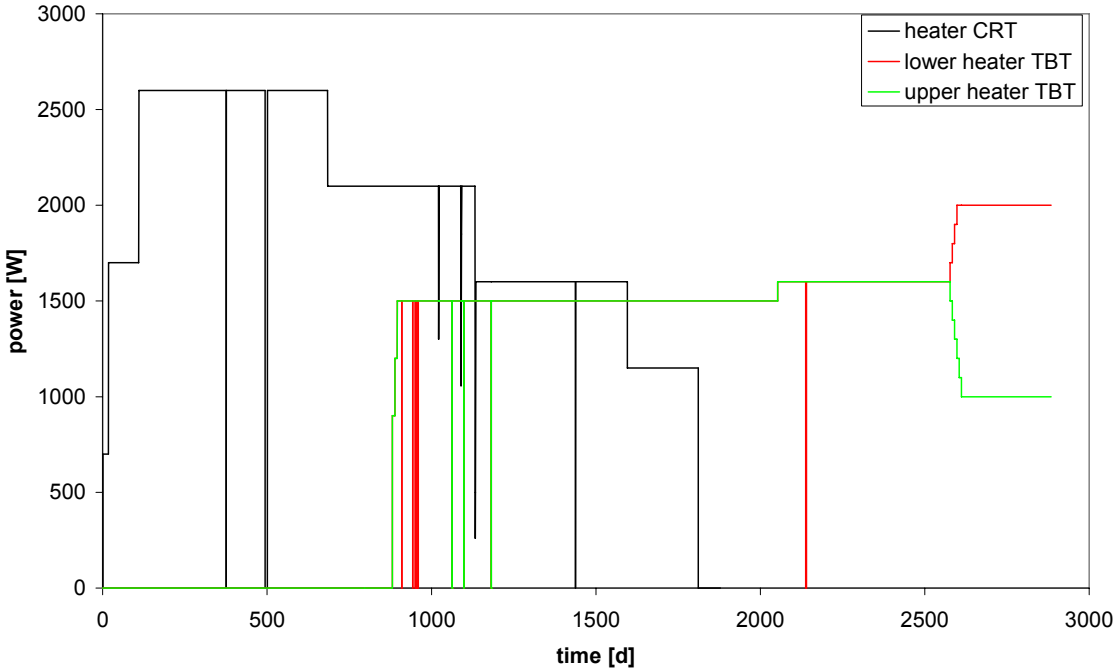

Figure 3-5. *Heat sources in the model.*

3.3 Parameter Values

For the bentonite materials the curves for the suction had been matched to the initial conditions with the equation:

$$s = c \ln(S_w) \qquad (1)$$

with

s: suction

c: constant

S_w: water saturation

Taking for example the bentonite rings in CRT with a suction value of 37 MPa at a water saturation of 0.849 the constant can be fitted with about $-2.26 \cdot 10^8$. The suction curves for the materials in the model are depicted in Figure 3-6.

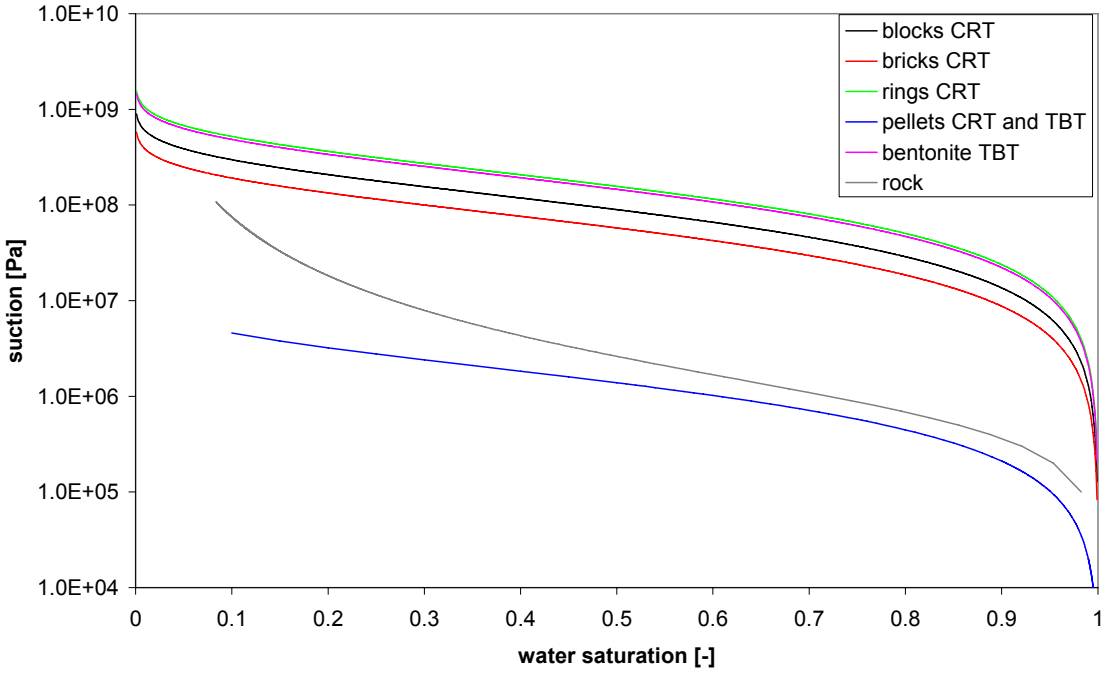

Figure 3-6. *Suction curves.*

The permeability values for the buffer were varied during the processing of this benchmark, see Table 3-3. This parameter has a strong influence on the predicted evolution of water saturation in the buffer. Another parameter which was varied is the tortuosity value which influences the vapour diffusion (SHAO & NOWAK 2008):

$$D_V = 2.16 \times 10^{-5} \tau S_g n (T_{abs} / 273.15)^{1.8} \quad (2)$$

with

D_V: vapour diffusion coefficient

τ: tortuosity [-]

S_g: gas saturation [-]

n: porosity [-]

T_{abs}: temperature [K]

Heat capacity of a porous medium is calculated according to the following equation:

$$c\rho = nS_w c_w \rho_w + n(1 - S_w) c_g \rho_g + (1 - n) c_s \rho_s \quad (3)$$

Heat conductivity of porous media except the buffer materials is calculated according to the following equation:

$$\lambda = nS_w \lambda_w + n(1 - S_w) \lambda_g + (1 - n) \lambda_s \quad (4)$$

with

c:	heat capacity of porous medium or (with index) of phase (solid, gas, water)
λ:	heat conductivity of porous medium or (with index) of phase
ρ:	density of porous medium or (with index) of phase
S:	phase saturation
n:	porosity

Heat conductivity of the buffer materials in CRT and TBT (except pellets) is approximated by a piecewise-linear function according to measured data, see Figure 3-7.

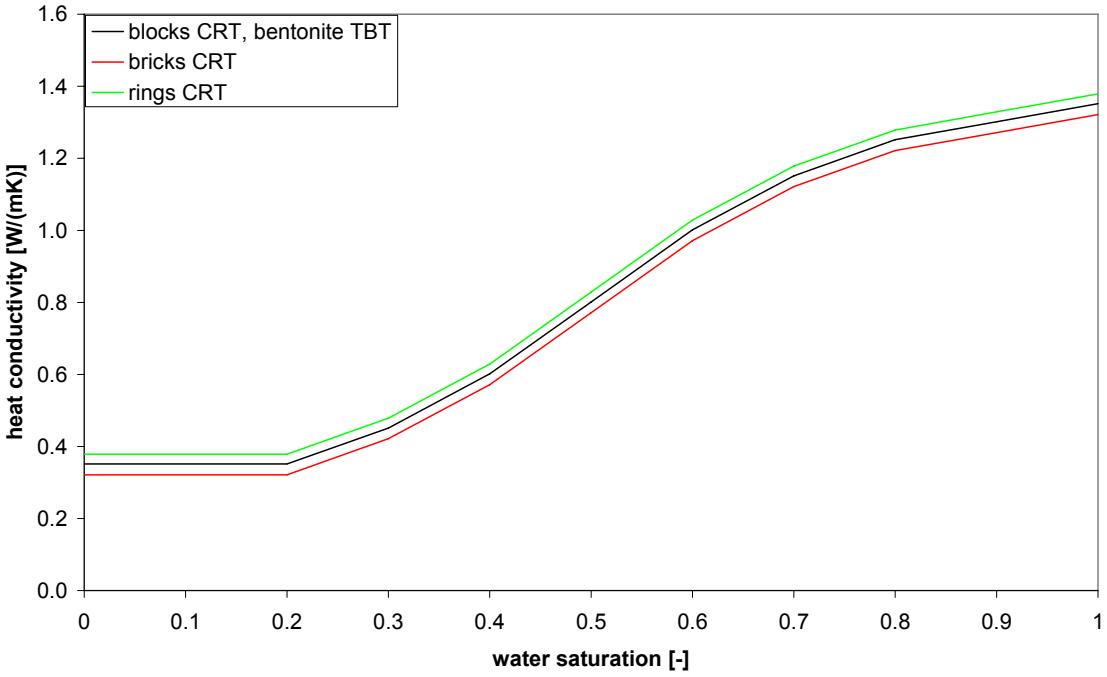

Figure 3-7. *Heat conductivity of buffer materials.*

With respect to thermal parameters the heat conductivity of the pellets was used as one fitting parameter. With the laboratory value of 1.0 W/(mK) the temperatures in the CRT buffer are overestimated. Instead a value of 1.28 W/(mK) is used. This fitting can be justified with the increasing dry density of the pellet layer due to the swelling of the inner bentonite bricks and rings. The thermal conductivity increases with dry density (compare Figure 3-7).

Another material which was adjusted with respect to thermal parameters is the one for the open excavations. The model does not include the ventilation of the galleries which causes a cooling of the rock. Instead the heat capacity and conductivity was increased to artificial values to account for the cooling effect.

Table 3-3 to Table 3-5 summarize the properties used in the calculations.

Table 3-3. Hydraulic properties.

	excavations	steel lids	concrete plugs	heaters	bentonite blocks	bentonite rings	bentonite bricks	bentonite pellets	granite	sand filter (TBT)	sand shield (TBT)	bentonite 1 (TBT)	bentonite 2 (TBT)
k [10^{-21}m²]	(no calculation of hydraulic processes)				2.9 (4.0)[3]	1.7 (3.0)[3]	4.8 (6.0)[3]	10	50	5E+4		4.5 (2.5)[4]	3.5 (1.5)[4]
n [-]					0.389	0.359	0.419	0.64	0.002	0.5		0.389	0.368
k_{rel} [-]					S^3								
-c [10^6]					129	226	83	[1]		[2]		210	210
τ [-]					0.4 (0.1; 0.6)[3]				-			0.4 (0.1; 0.6)[4]	
init. *s* [MPa]					37	37	37.5	0			0.007	47.5	47.5
init. *S* [-]					0.751	0.849	0.637	1			0.008	0.798	0.798

[1] see Figure 3-6
[2] very low suction (7000 Pa at 0.8% water saturation)
[3] parameter variation, compare chapter 4.4
[4] parameter variation, compare chapter 4.5

Table 3-4. Thermal properties.

	excavations	steel lids	concrete plugs	heaters	bentonite blocks	bentonite rings	bentonite bricks	bentonite pellets	granite	sand filter (TBT)	sand shield (TBT)	bentonite 1 (TBT)	bentonite 2 (TBT)
c_s [J/(kgK)]	1E+4	460	770	450	800				770	800			
λ_s [W/(mK)]	1E+5	47	2.7	100	[5]				2.6	1.9		[5]	
ρ_s [kg/m³]	1.19	7840	2400	8000	2780				2770	2780			

[5] see Figure 3-7

Table 3-5. Mechanical properties.

	excavations	steel lids	concrete plugs	heaters	bentonite blocks	bentonite rings	bentonite bricks	bentonite pellets	granite	sand filter (TBT)	sand shield (TBT)	bentonite 1 (TBT)	bentonite 2 (TBT)
E [GPa]	(no calculation of mechanical processes)	210	30	210	0.02		(not represented in the spatial discretisation)	(not represented in the spatial discretisation)	70	(not represented in the spatial discretisation)	0.02	0.02	
ν [-]		0.3	0.15	0.3	0.44				0.3		0.44	0.44	
p_{sw}^{max} [MPa]		-	-	-	10				2770		-	10	
α [10^{-5} K^{-1}]		1.2	1	1.2	0.3				0.38		0.3	0.3	

4 Results

In the following chapters results are shown only in time history plots both for CRT and TBT, whereas the comparison of calculated data for TBT with measured data had not been treated in the same depth as the CRT-results. In the figure legends the declaration in brackets (for example R5/A/585mm) refers to the bentonite ring or block (compare Figure 2-2), a certain direction, and the radius from the borehole centre.

With respect to hydraulic properties six calculation cases were performed with different permeability and tortuosity values (see chapter 4.4 and 4.5). Though thermal capacity and thermal conductivity depend strongly on water saturation, the resulting differences of these six calculations are of minor importance with respect to the temperature plots for CRT and the rock.

4.1 Temperatures in the rock

The measured temperatures in the rock at heater mid-height (symbols in Figure 4-2) are reproduced well by the calculation throughout the duration of CRT. Sensor TR120 and TR128 were located in vertical boreholes in 1.5 m distance from CRT's central axis, whereas TR128 was in a borehole in about the direction of TBT and TR120 on the opposite side, see Figure 4-1. Sensor TR117 and TR125 were on the borehole wall of CRT, TR125 (as TR128) in about TBT-direction. The calculated data is plotted in corresponding colours with lines.

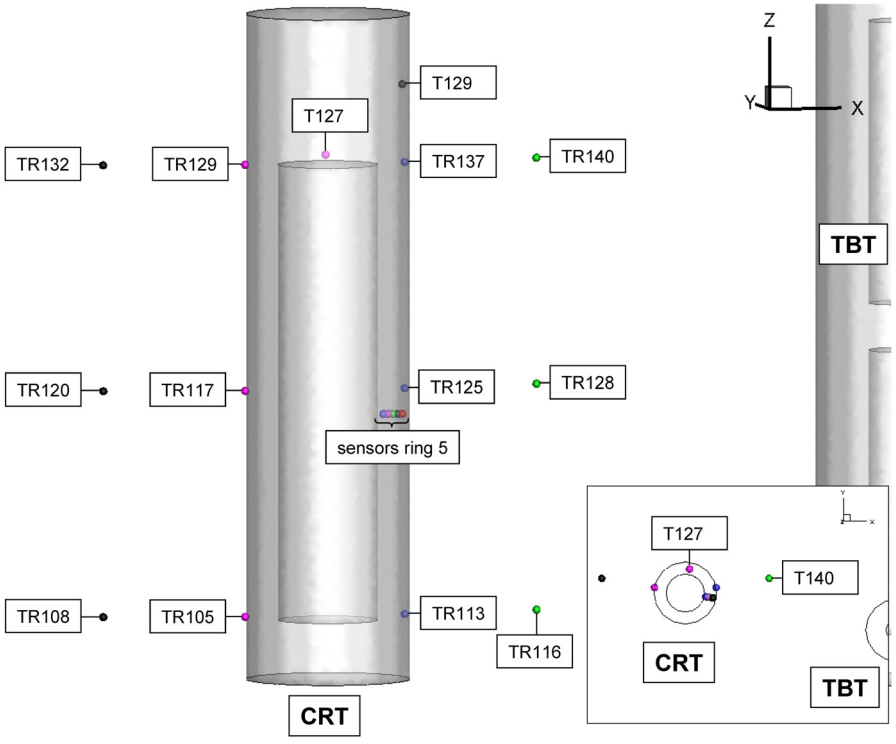

Figure 4-1. *Temperature sensor positions in rock and CRT.*

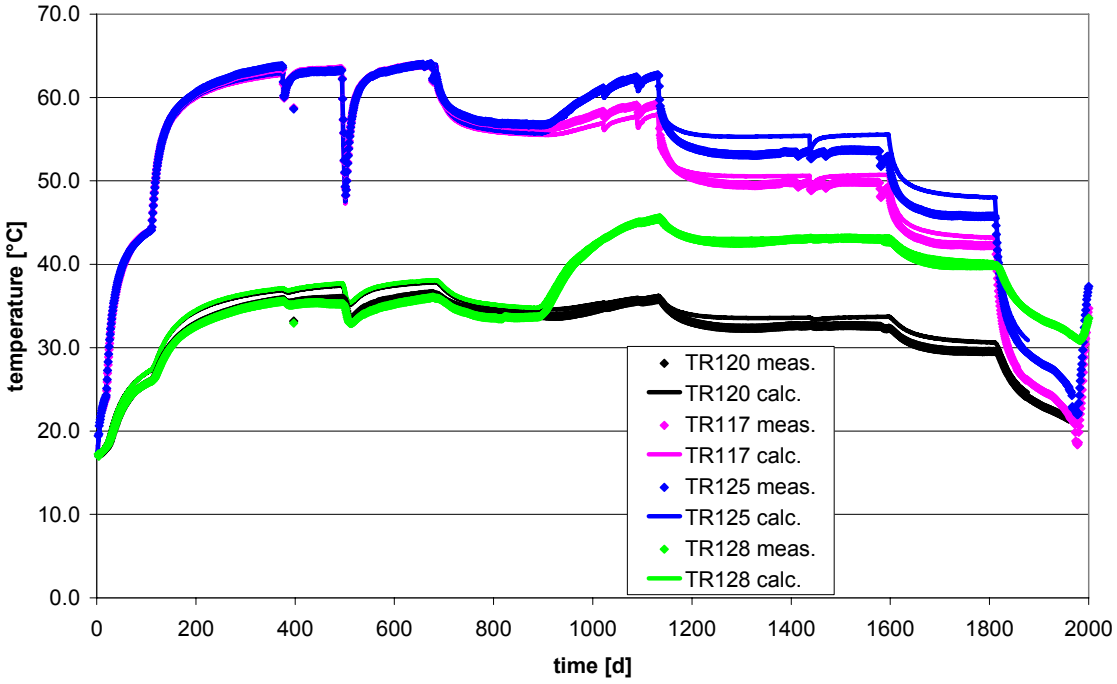

Figure 4-2. *Temperatures in the rock at heater mid-height.*

The measured temperatures in the rock at the height of heater top and bottom are not reproduced as well as at heater mid-height, but still fairly well.

At heater top (see Figure 4-3) the temperatures are slightly underestimated by the calculation which might be attributed to some extent to the artificially raised heat conductivity and capacity of the open excavations which is meant to take into account the cooling by ventilation.

At heater bottom (see Figure 4-4) the temperatures are slightly overestimated by the calculation for the sensors TR108 and TR116 which are 1.5 m from CRT's central axis. For the sensors TR105 and TR113 at the wall of the deposition hole the temperatures are underestimated by the calculation.

Discontinuities in the rock might contribute to a heat transport regime which differs locally significant from the calculation where heat transport is governed by heat conduction in a porous, low permeable, homogeneous rock.

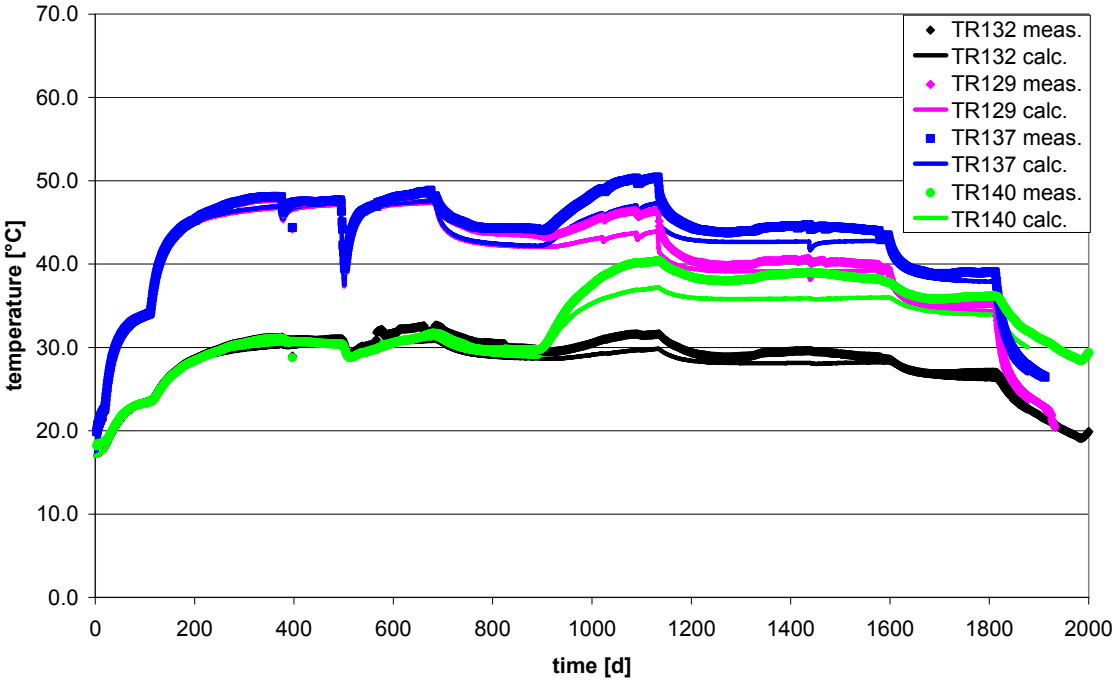

Figure 4-3. *Temperatures in the rock at heater top.*

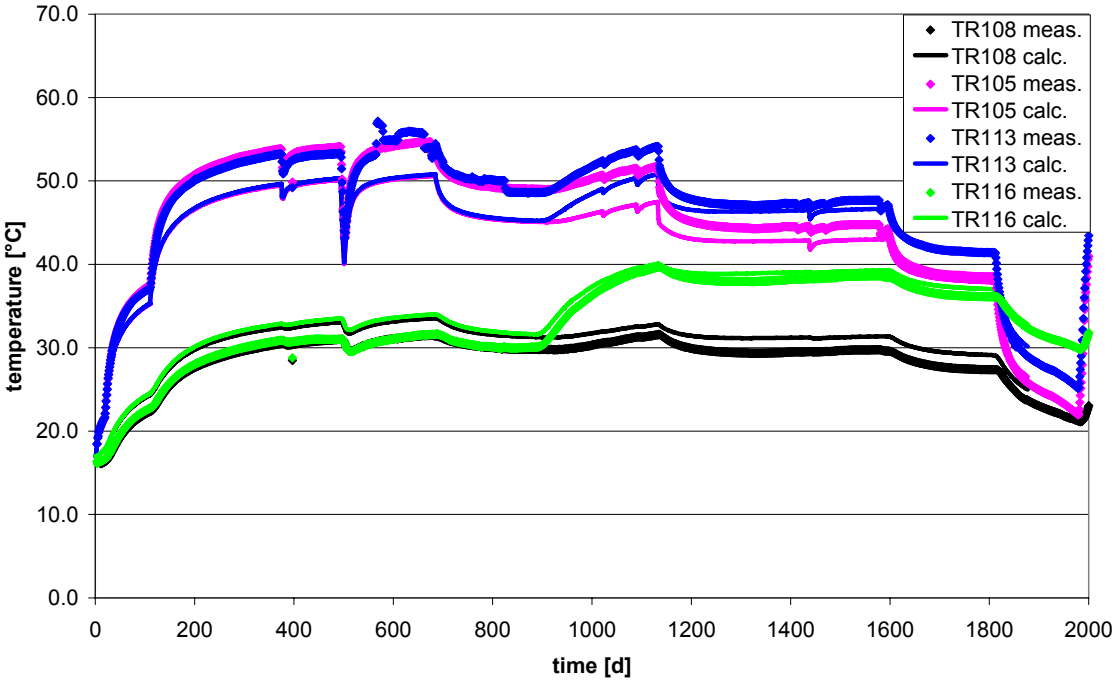

Figure 4-4. *Temperatures in the rock at heater bottom.*

4.2 Temperatures in CRT

At heater mid-height in bentonite ring R5 temperature was measured at five positions, see symbols in Figure 4-5. The calculated data is plotted in corresponding colours with lines. For sensor positions refer to Figure 4-1 (labelled “sensors ring 5”).

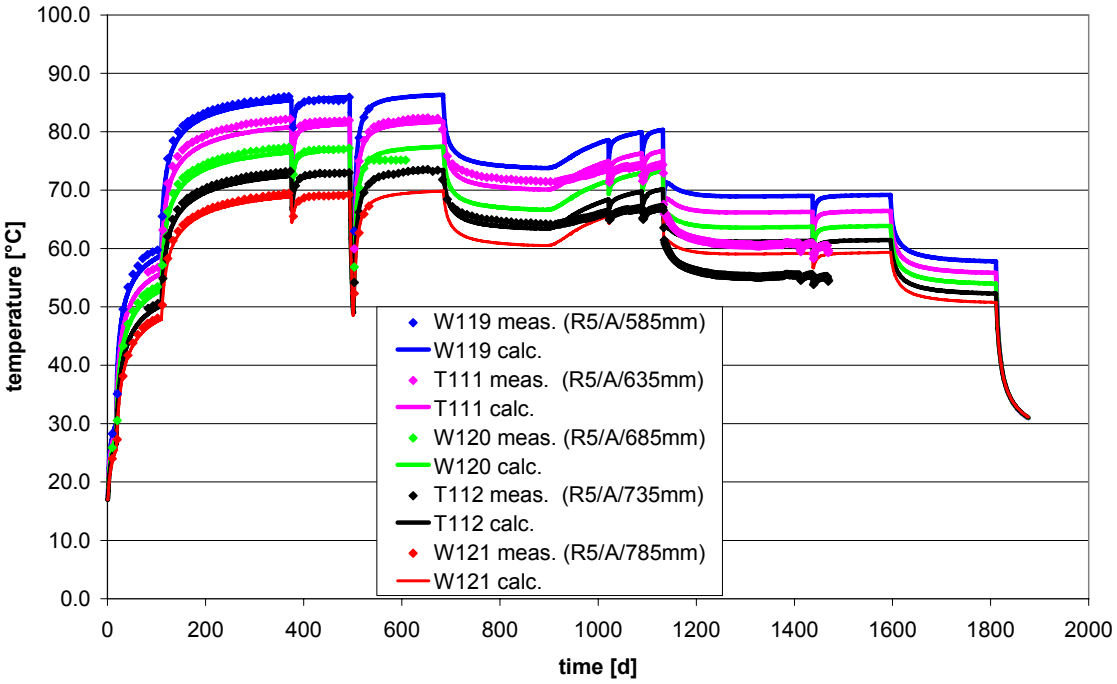

Figure 4-5. *Temperatures in CRT in ring 5.*

Until the TBT-heaters are switched on in the model after roughly 900 days the measured temperatures are reproduced well (deviation of 1.5°C at maximum) with the calculation, especially the events with a loss of heater power after roughly 380 days and after 500 days. After the TBT-heaters are switched on, the deviation increases significantly.

The calculated temperature at sensor T129 in block 3 (black line in Figure 4-6) fits well to the measured temperature (black symbols). For sensor T127 in ring 10 (magenta symbols) the agreement between calculation and measured data increases towards the end of the test.

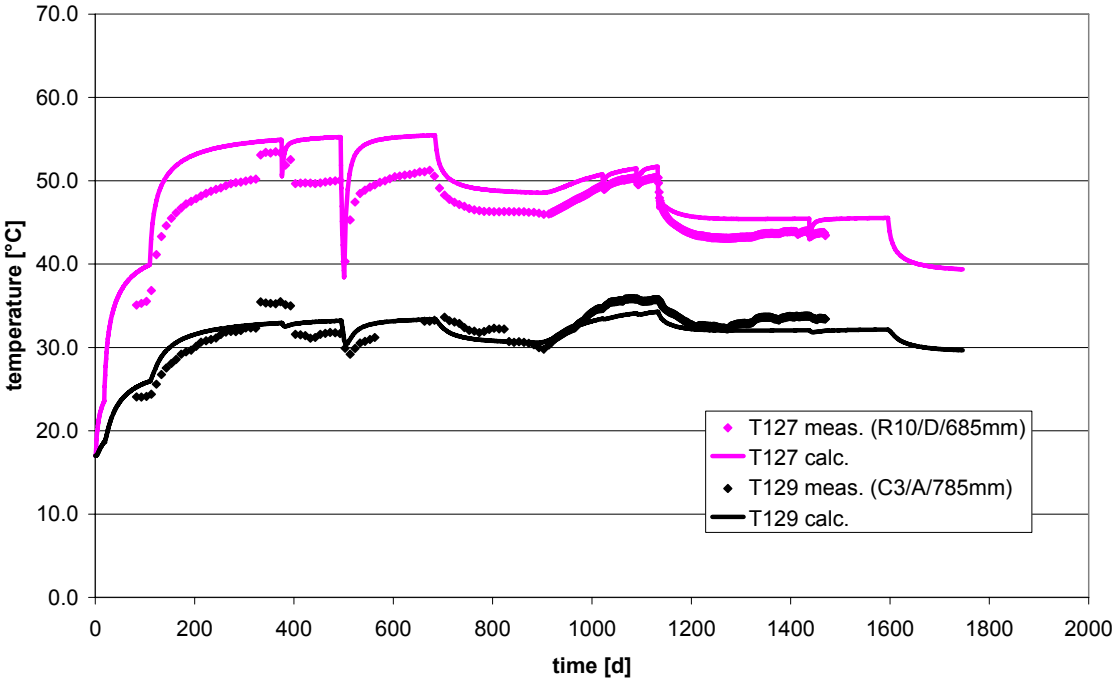

Figure 4-6. *Temperatures in CRT in ring 10 and block 3.*

4.3 Temperatures in TBT

For TBT the calculated temperature data reproduces the measured data not as well as for CRT and the rock.

Figure 4-8 shows a comparison of measured and calculated temperature at one position on the (lower) heater no. 1 (black symbols) and one position on the (upper) heater no. 2 (red symbols) where the agreement between measured and calculated data is best. For sensor positions in TBT refer to Figure 4-7. For other temperature sensors the disagreement between calculated and measured data is higher without a clear tendency of the calculation to over- or underestimate the measured temperature.

The time axis of the diagrams in this chapter is labelled as TBT-time which refers to the starting of the heaters in TBT (compare Table 3-2). Figure 4-9 shows a comparison of measured and calculated temperature at several positions in the buffer. The calculated temperatures are too low in comparison to the measured values. In the modelling work to TBT reported by ÅKESSON (2006) the heat conductivity of the bentonite is modelled to range between 0.3 W/(mK) in dry state and 1.25 W/(mK) in saturated state. In comparison in the model described here the heat conductivity ranges between 0.38 W/(mK) and 1.38 W/(mK) according to the measured values, see Figure 3-7.

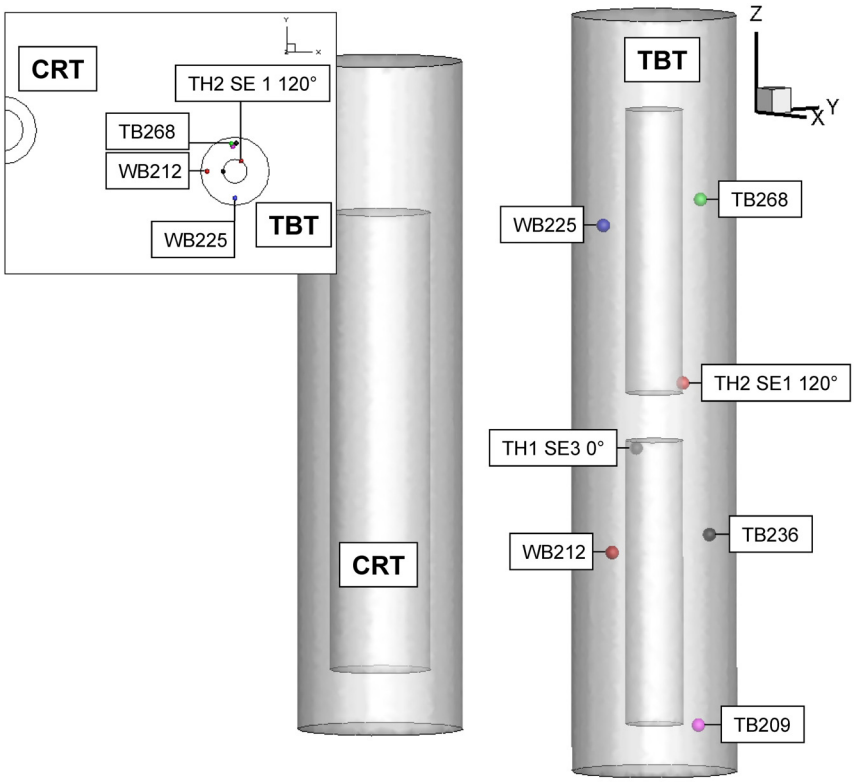

Figure 4-7. *Temperature sensor positions in TBT.*

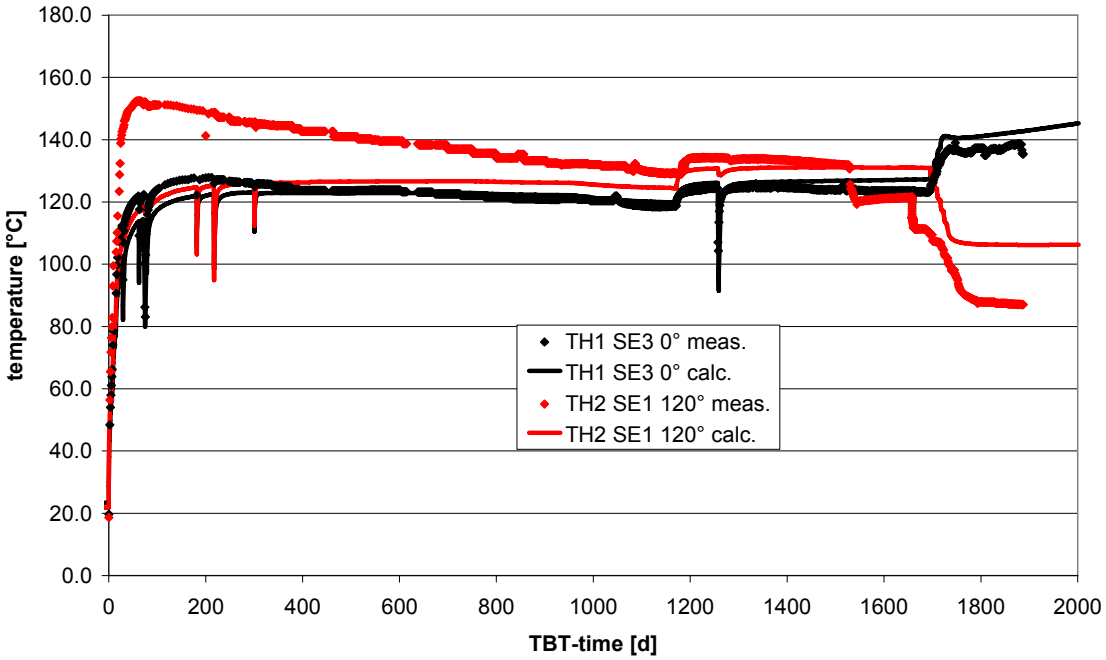

Figure 4-8. *Temperatures in TBT at upper and lower heater.*

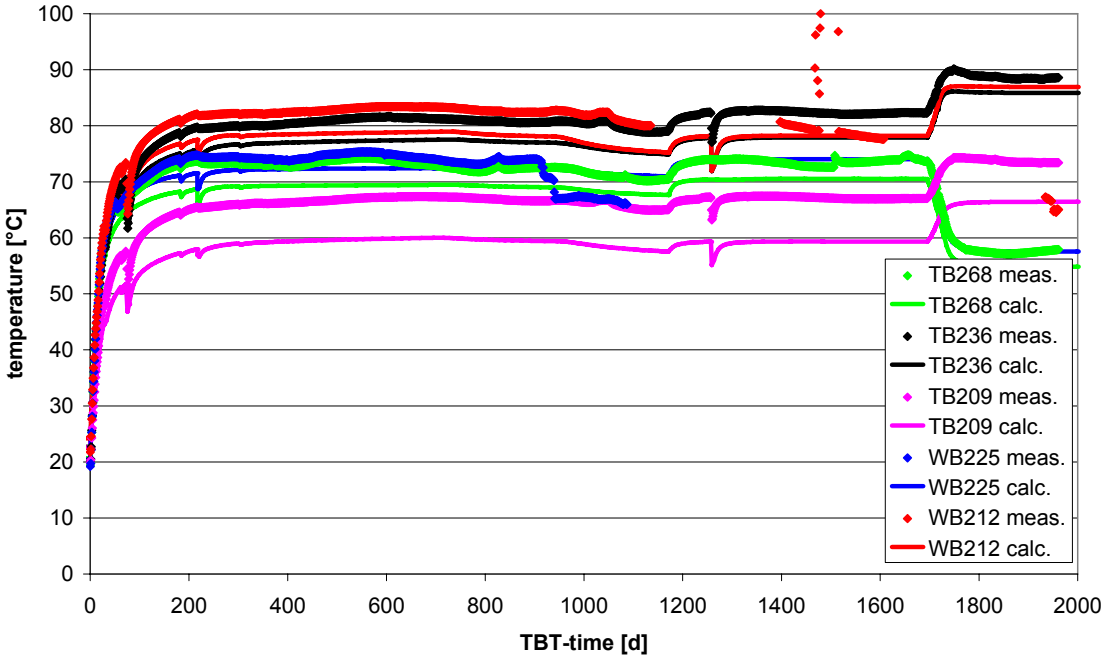

Figure 4-9. *Temperatures in TBT at several positions in the buffer.*

4.4 Suction and relative humidity in CRT

The distribution of water in the buffer materials of CRT was measured with sensors for suction and sensors for relative humidity. For sensor positions in the following plots refer to Figure 4-10 (labelled "sensors ring 5"). Six calculations were performed using two sets of permeability values for the buffer materials and three different tortuosity values, compare Table 3-3. Permeability values had been determined in the laboratory and the values used in the calculations were within the determined range. The tortuosity value which is used in an empirical relationship for the vapour diffusion coefficient was set as 0.1, 0.4 (as in BM 1.1.1, compare NOWAK 2007), and 0.6.

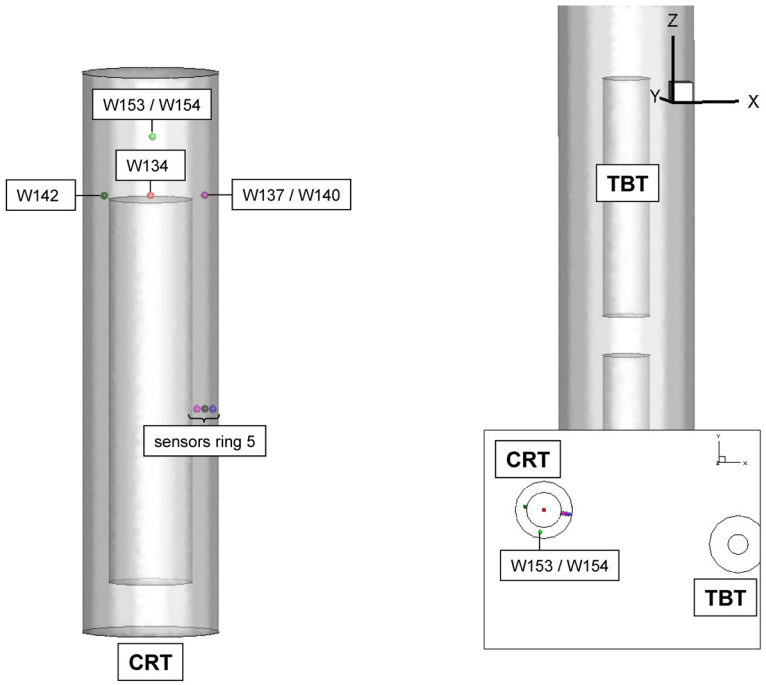

Figure 4-10. *Suction and relative humidity sensor positions in CRT.*

The first set of comparing plots is for the relative humidity sensors in ring 5. Figure 4-11 shows the results for the calculation with low permeability values and Figure 4-12 for the slightly increased permeability values.

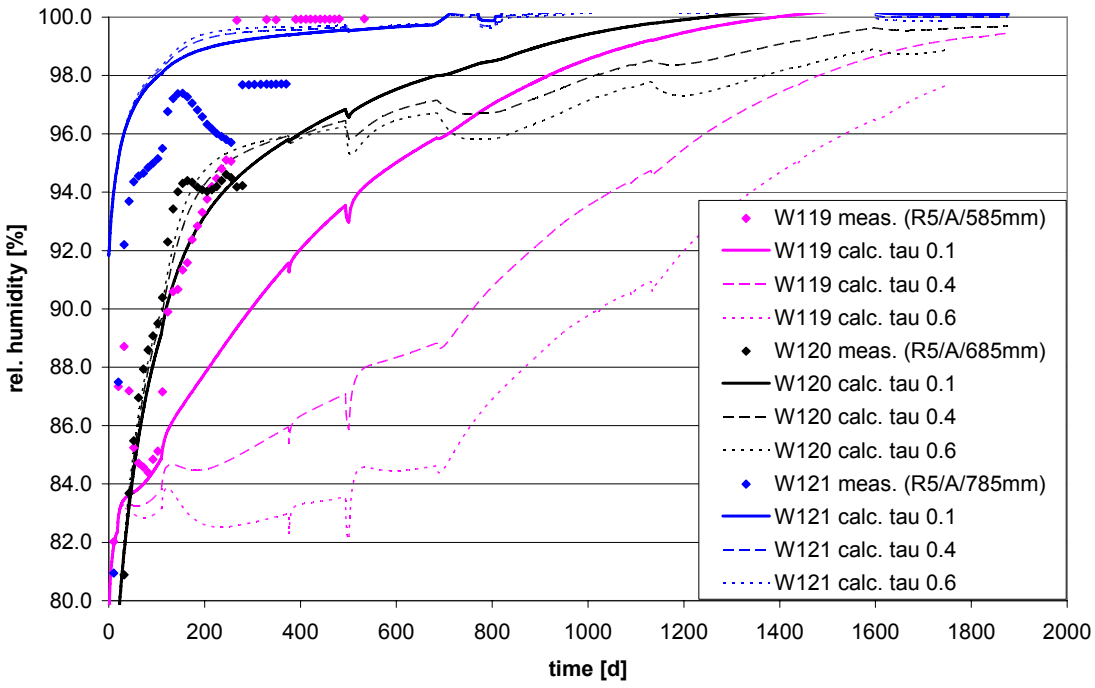

Figure 4-11. *Relative humidity in CRT in ring 5, low permeability.*

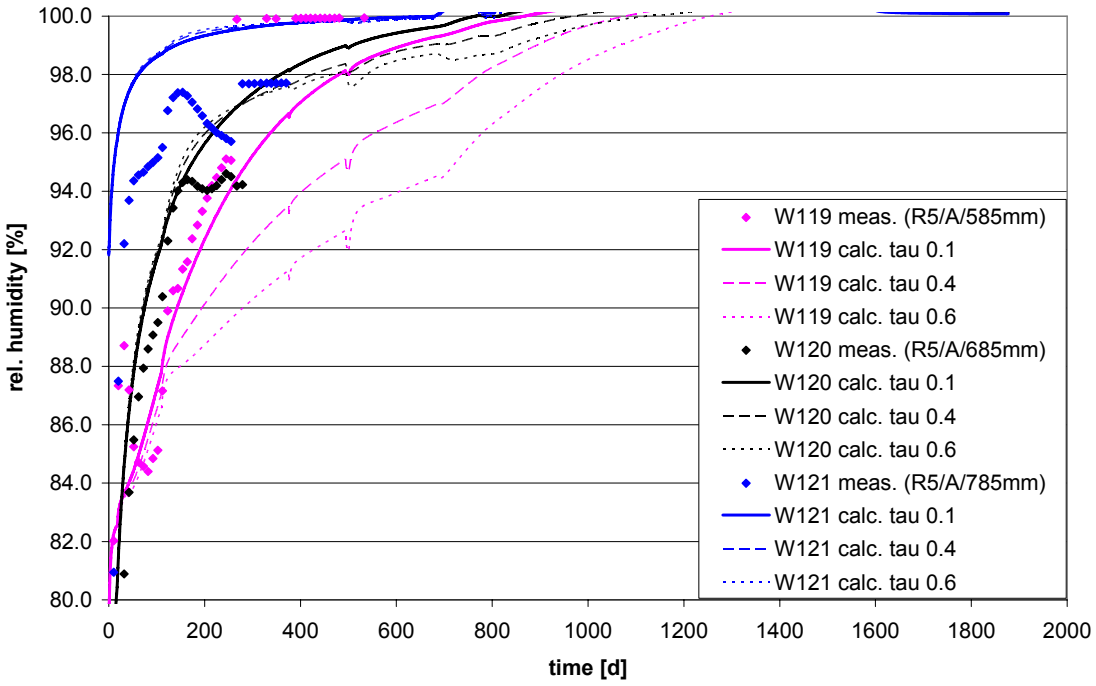

Figure 4-12. *Relative humidity in CRT in ring 5, slightly increased permeability.*

For sensor W121 near the borehole wall the variation of tortuosity hardly changes the calculated results indicating that the saturation process in the calculation is governed by the movement of the fluid phase. All calculation cases overestimate the saturation progress.

The measured data from sensor W120 shows in the beginning a fast increase until a value of about 94% is reached. This fast increase is followed by a period of about invariant values until the sensor fails. The calculated values for the low permeability case (Figure 4-11) show within this period also a slow-down of the saturation progress. The higher the tortuosity value the more pronounced the slow-down is. In general the influence of tortuosity is more pronounced in the low permeability calculation cases in comparison to the cases with the increased permeability. The calculated values are in the correct range. The calculation cases with the slightly increased permeability (Figure 4-12) tend to overestimate the saturation progress for this sensor, but the calculated values are in the correct range for the period of the fast increase in the beginning.

The measured data from sensor W119 which is nearest to the heater shows not only the same tendency as the sensors further away from the heater but also the same order of magnitude for the measured relative humidity. The value gets even higher as the value for the sensor W120. As discussed in chapter 2.1 there was an inner construction gap between heater and bentonite rings which might have been filled with water during the filling of the outer gap via flow along construction interfaces. For this reason the initial hydraulic state of the rings in the calculation as stated in Table 3-3 might not be completely in compliance with the experiment and then explain the misfit between calculation and measured data. Only the calculation case with the increased permeability value and a tortuosity of 0.1 gives values which agree with the measured data, the other calculation cases underestimate the saturation progress. In the model there is no inner construction gap and the heater is in contact with the bentonite rings from the beginning.

The second set of comparing plots is for suction in ring 5. Figure 4-13 shows for the calculation with low permeability values the same calculated results as in the previous two diagrams, but in terms of suction. Figure 4-14 is for the slightly increased permeability values.

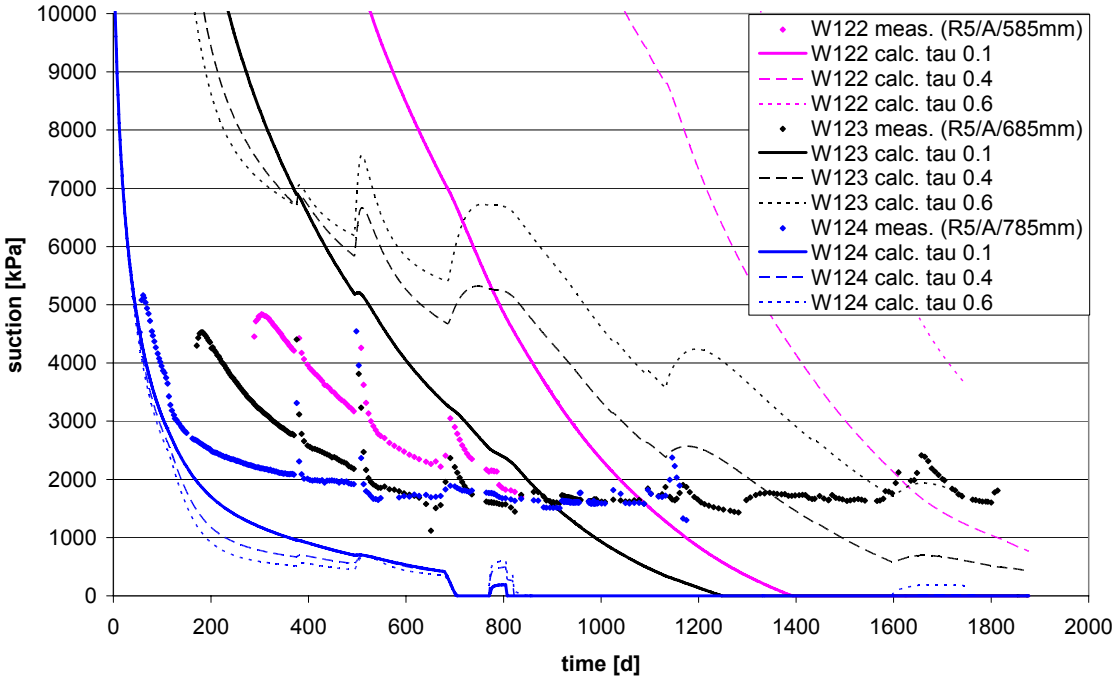

Figure 4-13. *Suction in CRT in ring 5, low permeability.*

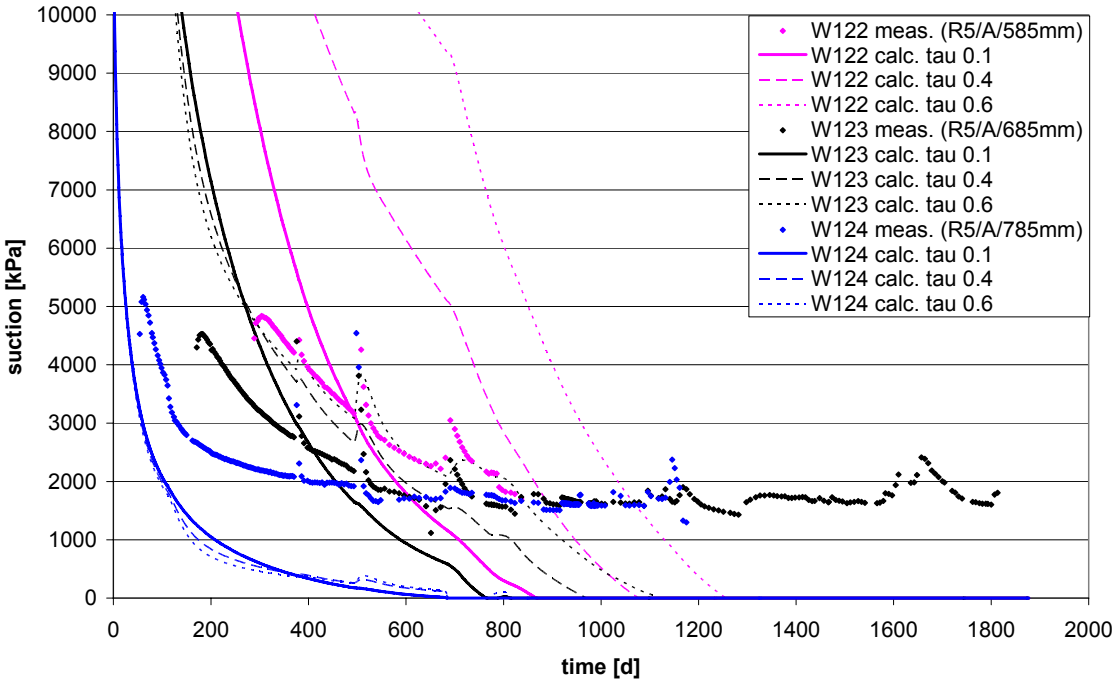

Figure 4-14. *Suction in CRT in ring 5, slightly increased permeability.*

For the suction sensors an indication of well above 1000 kPa suction remains in case of full saturation which does not allow for a direct comparison of measured and calculated data. The same tendency of over- or underestimation of the saturation progress as discussed for the relative humidity sensors is also valid for the suction sensors. Sensor W122 fails after about 800 d when reaching the indication of full saturation. The calculation case with the increased permeability and the tortuosity of 0.1 shows full saturation at this sensor after about the same time. This parameter set gave also the best agreement for the relative humidity sensor W119 (Figure 4-12).

The third set of comparing plots is for two relative humidity sensors in ring 10 and one in block 3. Figure 4-15 shows the results for the calculation cases with low permeability values and Figure 4-16 for the cases with slightly increased permeability values.

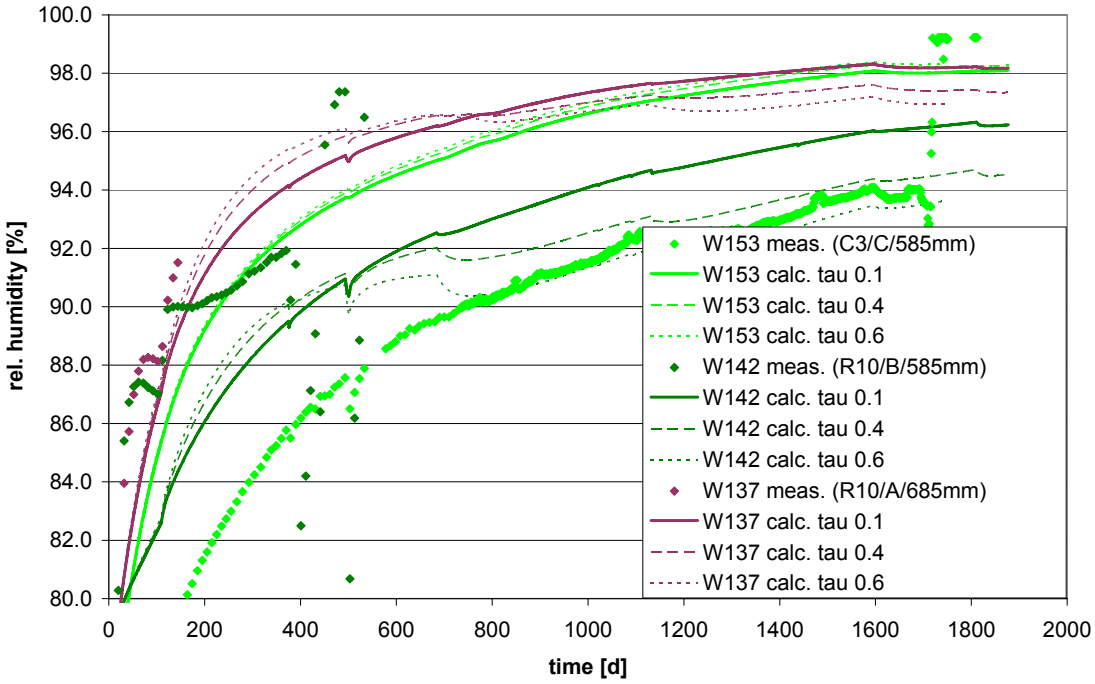

Figure 4-15. *Relative humidity in CRT in ring 10 and block 3, low permeability.*

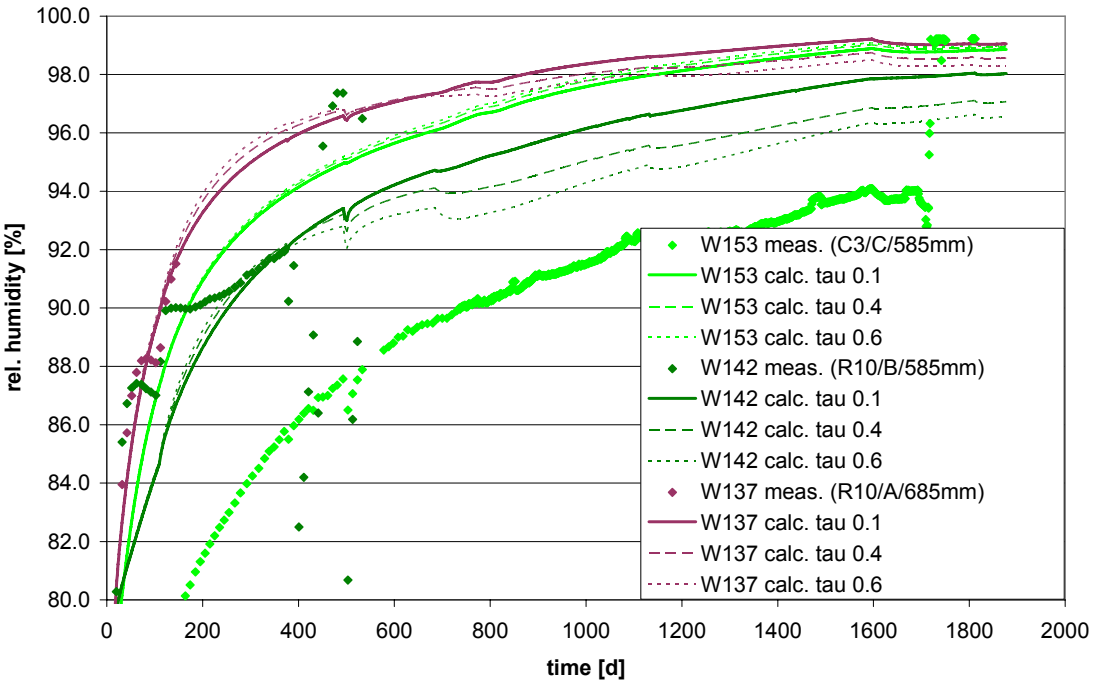

Figure 4-16. *Rel. humidity in CRT in ring 10 and block 3, slightly incr. Permeability.*

Sensor W153 is located more than a half metre above the upper edge of the heater. Tortuosity (vapour transport) hardly influences the calculated evolution of relative humidity at this sensor. Except for the measured values at the end of the test the calculated values do not fit the measured data with respect to the absolute value. When considering the evolution at that sensor as a rate (change of relative humidity per time unit) the calculation gives about the same relative humidity change per time unit (compare shape of measured and calculated evolutions).

W137 is located in the same radial distance from the heater as W120 (see for example Figure 4-11), but at height of the upper edge of the heater. In the same way W142 compares to W119. With respect to the discussion of agreement between calculated and measured data the same statements as for sensor W120 also hold for W137 and those for W119 for W142, respectively.

The fourth set of comparing plots is for one suction sensor in ring 10 and one in block 3. Figure 4-17 shows in terms of suction the same calculated results as in Figure 4-15 and Figure 4-18 in terms of suction the same calculated results as in Figure 4-16 for the slightly increased permeability values.

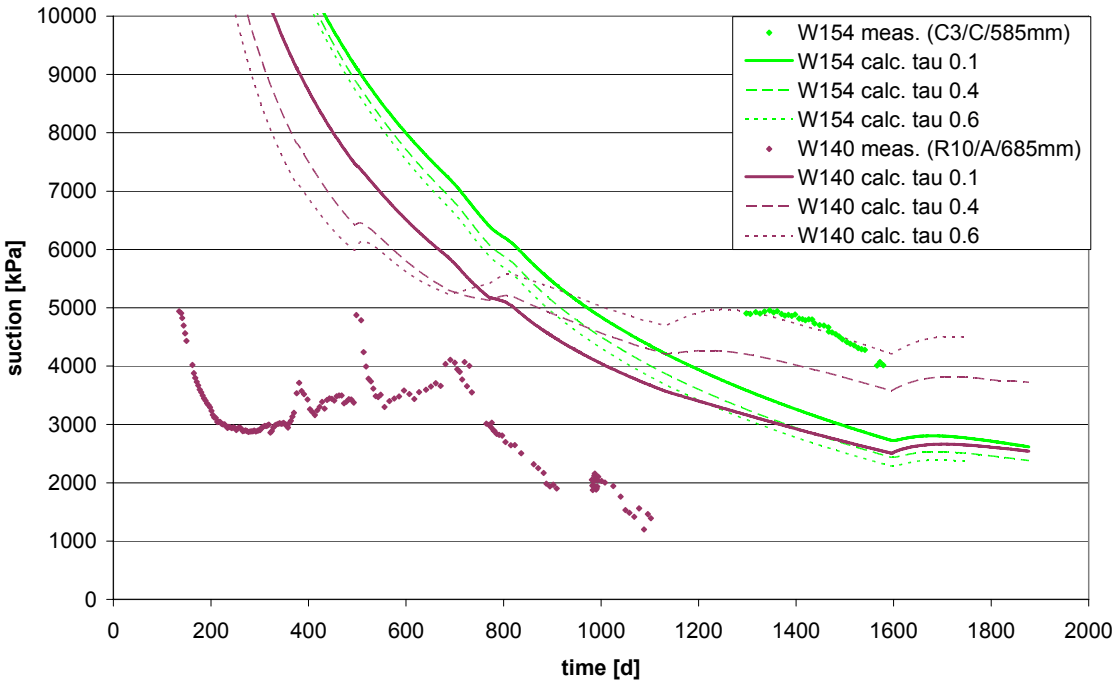

Figure 4-17. *Suction in CRT in ring 10 and block 3, low permeability.*

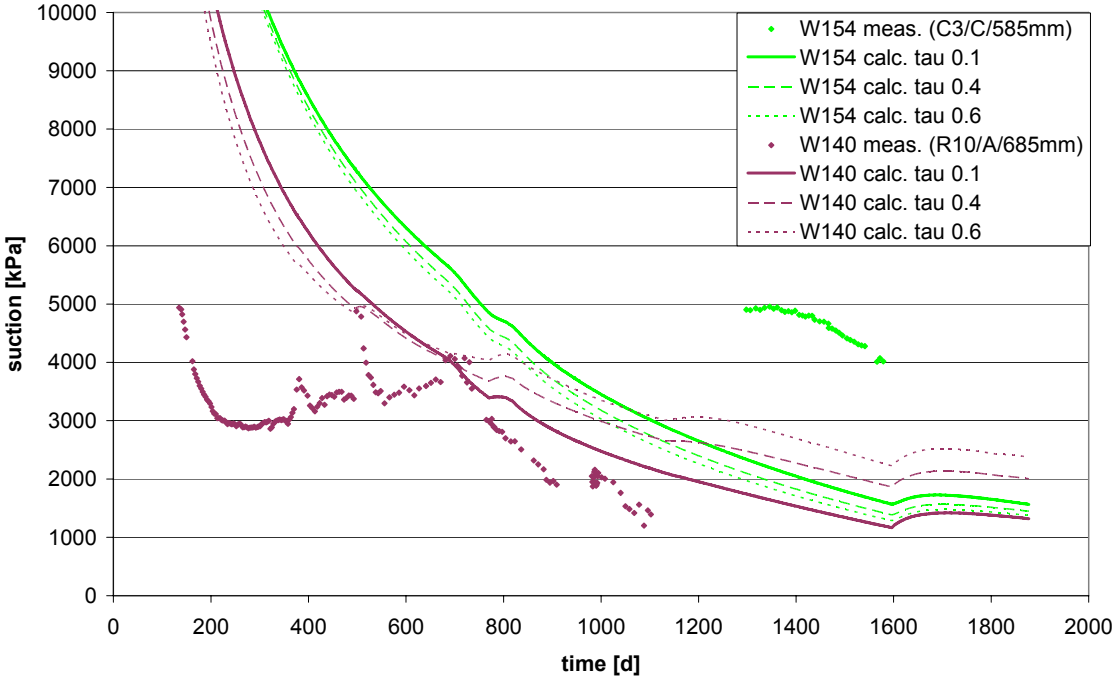

Figure 4-18. *Suction in CRT in ring 10 and block 3, slightly increased permeability.*

Calculated data for sensor W140 shows for all calculations cases an underestimation of the saturation progress. Only the calculation cases with slightly increased permeability show over the time period beginning around day 700 until sensor failure a quantitative agreement. On the other hand, calculated data for sensor W154 shows for all calculation cases an overestimation of the saturation progress.

The last pair of comparing plots is for the relative humidity sensor W134 in the center of ring 10 which shows some drying of the buffer material over a longer time period and at the end of the test a value which is about the initial state, see red symbols in Figure 4-19 and Figure 4-20.

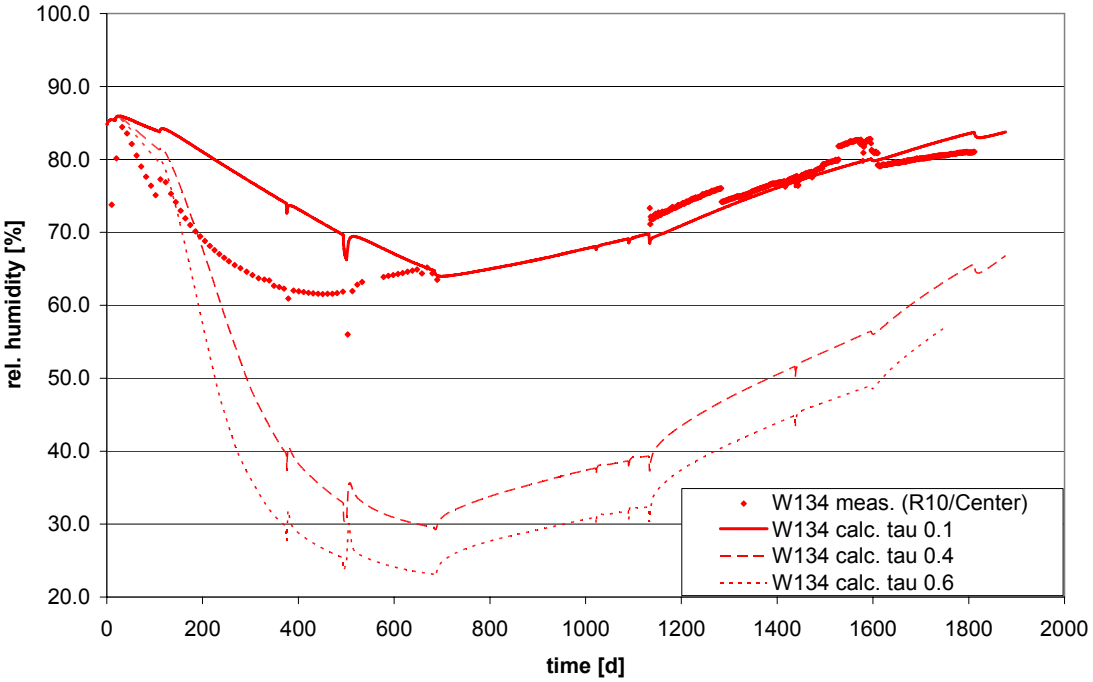

Figure 4-19. *Relative humidity in CRT at sensor W134, low permeability.*

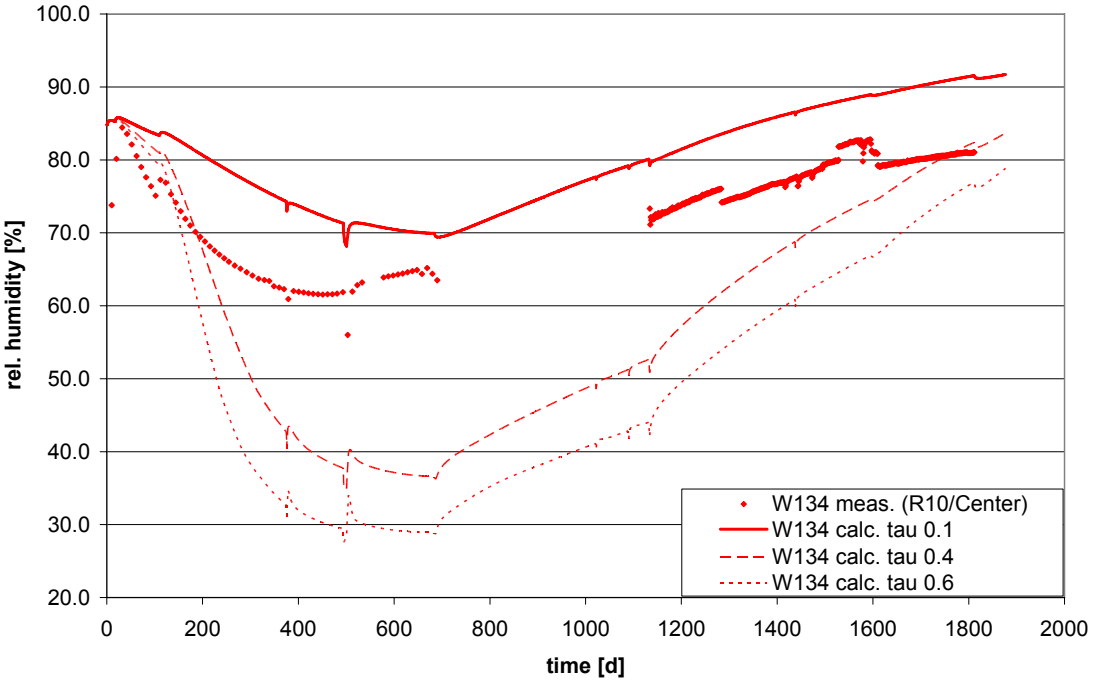

Figure 4-20. *Rel. humidity in CRT at sensor W134, slightly increased permeability.*

The calculated values for all six calculation cases reproduce this drying and re-wetting cycle qualitatively. The measured values show some events with a sudden, small decrease of relative humidity, best seen at days 379 and 503. These coincide with the events of heater power loss (compare Figure 3-5) which can also be recognized in all temperature evolution plots for CRT (see chapter 4.2). This phenomenon is also reproduced very well with all calculation cases.

The measured values are reproduced quantitatively in the calculation case with low permeability and a low tortuosity value of 0.1. With tortuosity values of 0.4 and 0.6 the calculated minimum of relative humidity is too low in comparison to the measured minimum for both sets of permeability values. The calculation cases with the lower permeability values also give the lower minimum in comparison to the calculation cases with slightly increased permeability values.

4.5 Suction and relative humidity in TBT

For the distribution of water in the buffer materials of TBT calculated data was compared to measured values from four relative humidity sensors. For sensor positions in the following plots refer to Figure 4-21. As for CRT six calculations were performed using two sets of permeability values for the buffer materials and three different tortuosity values, compare Table 3-3. The first set of permeability values - in the following named case 1 - was taken from the modelling work reported in ÅKESSON (2006). As these values for case 1 compare to the case with slightly increased permeability values for CRT, a second set of slightly decreased permeability values was investigated as case 2 (numbers in brackets in Table 3-3).

The time axis of the diagrams in this chapter is labelled as TBT-time which refers to the starting of the heaters in TBT (compare Table 3-2), which is day 881 of CRT. The modelled (instantaneous) emplacement of the TBT buffer materials is at day 796, this is in terms of TBT-time day -85. Figure 4-22 shows the comparison of calculated and measured data for case 1, Figure 4-23 for case 2.

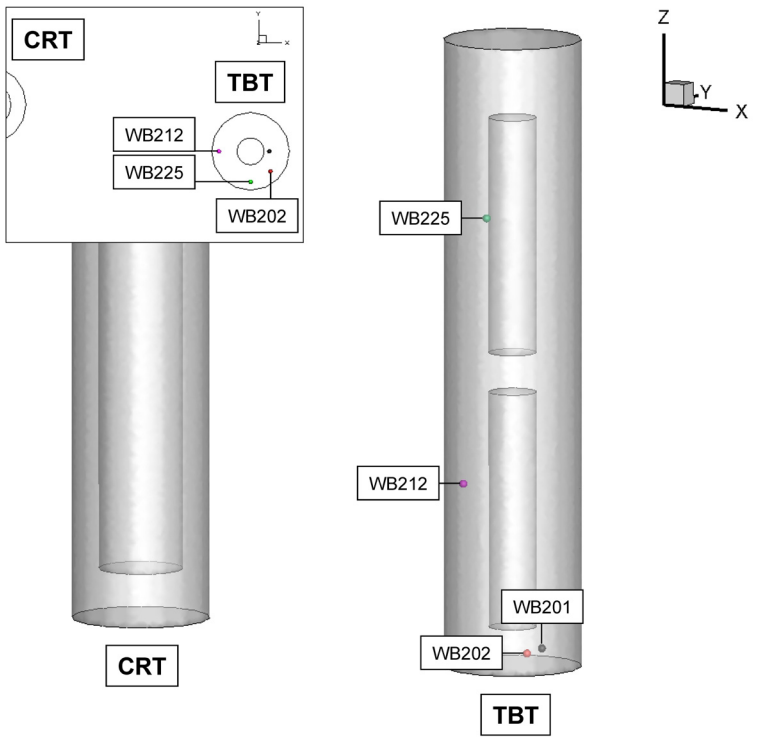

Figure 4-21. *Relative humidity sensor positions in TBT.*

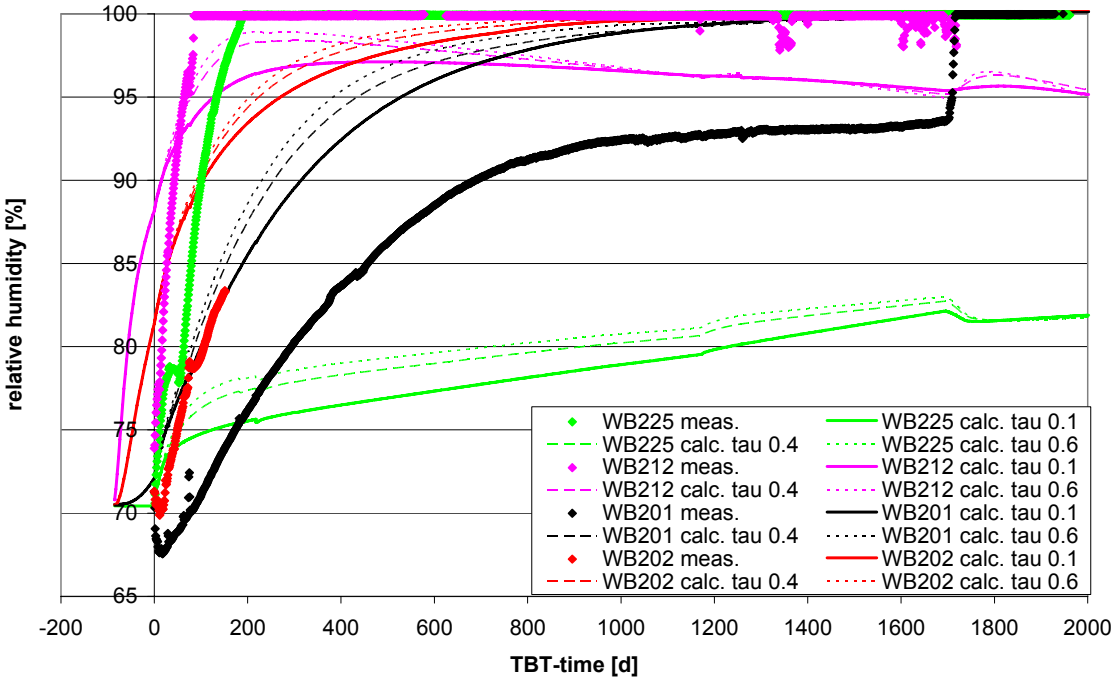

Figure 4-22. *Relative humidity in TBT, permeability case 1.*

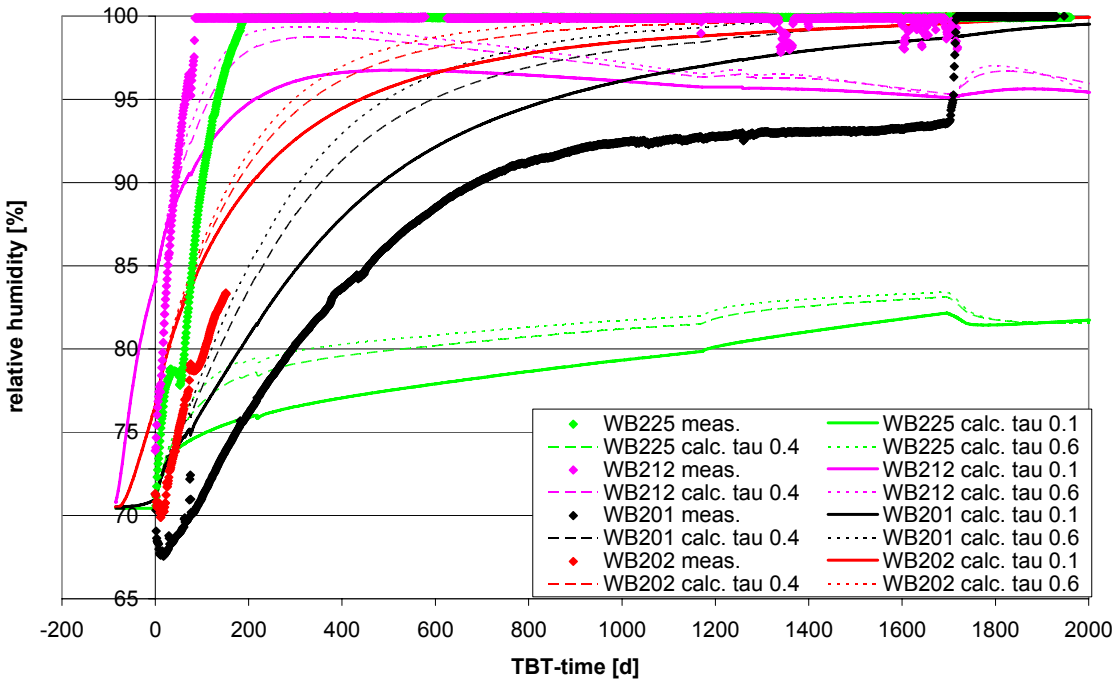

Figure 4-23. *Relative humidity in TBT, permeability case 2.*

The artificial saturation of TBT was done via a sand filter in the outer gap between the rock and the bentonite. The hydraulic state of that filter was modelled with the hydraulic boundary condition as given in Figure 3-3. At installation the curve starts at -7000 Pa which corresponds to a nearly dry sand filter (compare Table 3-3). Using the suction curve for the TBT-bentonite (see Figure 3-6), -7000 Pa correspond to a nearly water saturated state. For this reason the saturation process in the model starts earlier as in the real experiment.

Taking into account the shifted start of the artificial saturation, the measured evolution of relative humidity is reproduced well for three of the sensors and poor for WB225. When considering the evolution at sensor WB201 and WB202 as a rate (change of relative humidity per time unit) the calculation gives about the same relative humidity change per time unit (compare shape of measured and calculated evolutions in Figure 4-23). The measured data from WB212 gives a weak indication that relative humidity starts to drop after 1200 days TBT-time. The calculated data for all permeability and tortuosity cases shows that relative humidity reaches a maximum in the first half of the calculated time and then falls again. Considering the weakness of relative humidity sensors to measure high values of relative humidity the calculated data of sensor WB212 at least shows a qualitative agreement to the measured data.

For sensor WB225 the agreement of calculated data with the measured data is poor.

4.6 Total pressure in CRT

During the processing of this benchmark different spatial discretisations were used. In the first approach 2008 the outer layer of bentonite pellets was not taken into account and instead the bentonite rings and blocks were simplified in direct contact with the borehole wall. As a consequence the confinement of the bentonite blocks and rings was modelled too stiff. When the correct coefficient for maximum swelling pressure is used in the model, the predicted swelling pressure in the buffer is systematically too high.

In comparison to subsequent discretisations this first approach has to be considered as coarsely discretised. Finer discretisations which followed this first approach caused severe problems in the post-processing of the results. Finally not all of them turned out to be testable for the correct transfer of the input data into the numerical model and were not evaluable with the available post-processing tools. For this reason it was finally decided to discard all results from these calculations and to present only some of the results from the first approach without further discussion.

Sensor positions are shown in Figure 4-24. Figure 4-25 shows the comparison of measured and calculated data for sensor P111 in ring 5 (sensors ring 5, black (middle) symbol in Figure 4-24). Figure 4-26 shows the comparison for the sensor P125 in block 3 and P119 in ring 10.

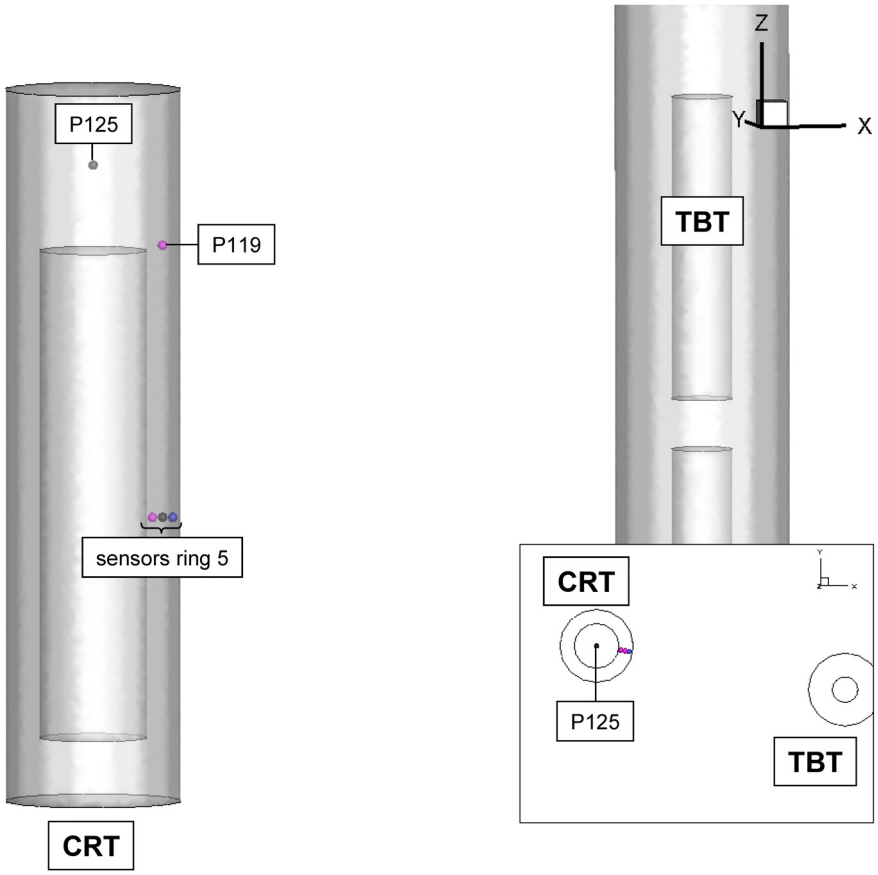

Figure 4-24. *Total pressure sensor positions in CRT.*

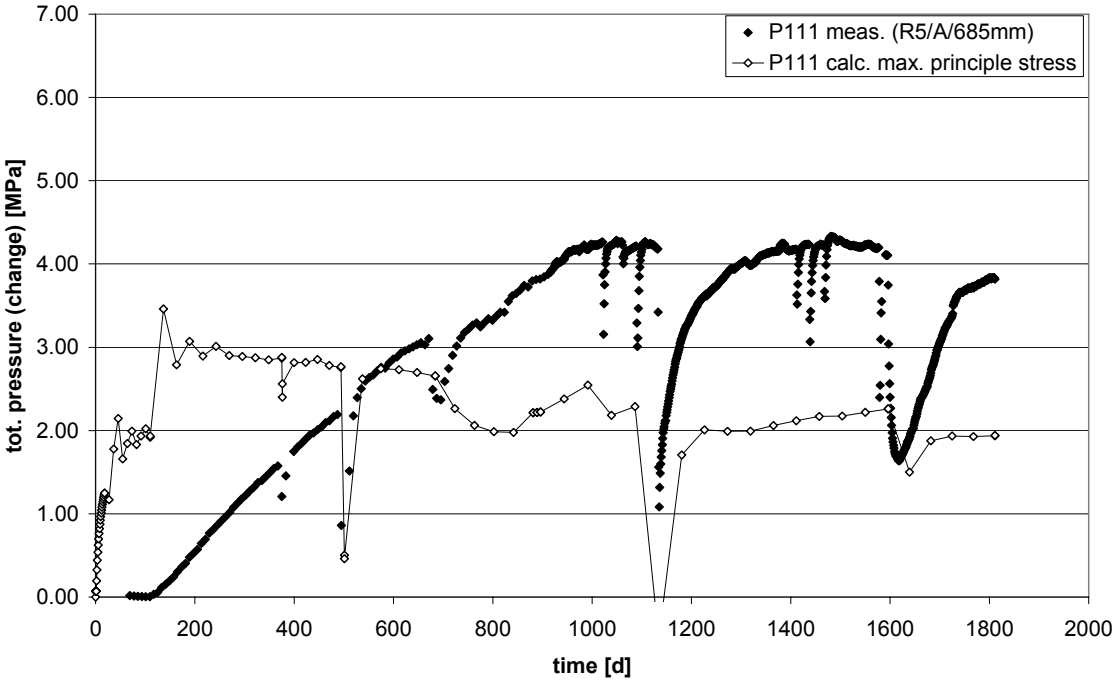

Figure 4-25. *Total pressure for sensor P111 in ring 5.*

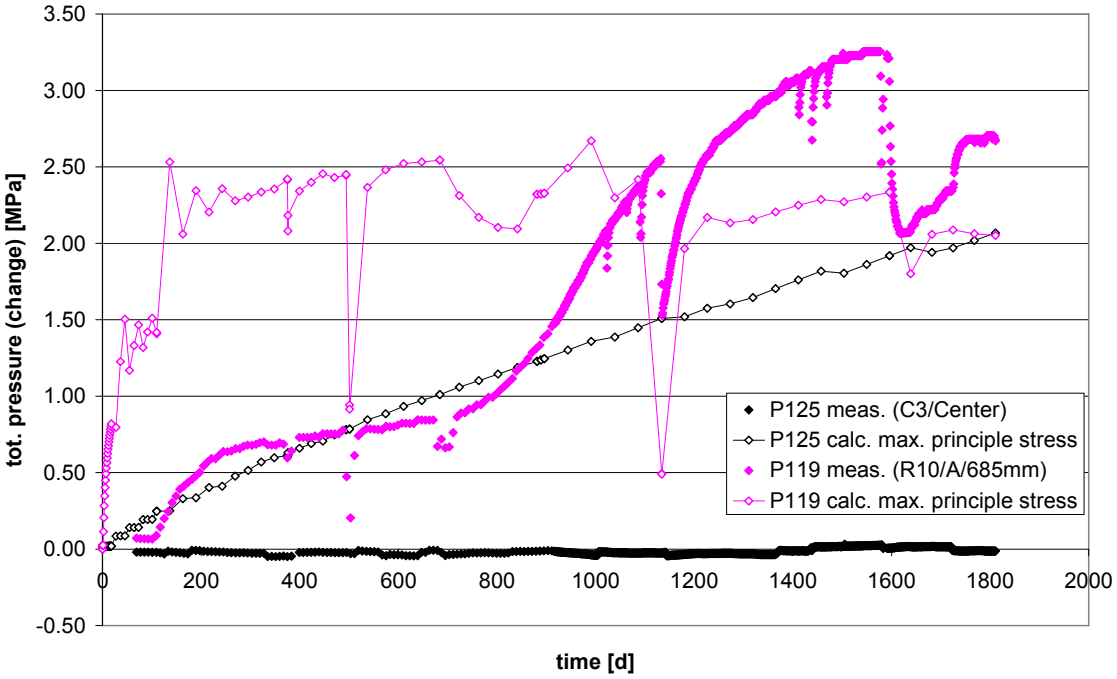

Figure 4-26. *Total pressure for sensors P125 in block 3 and P119 in ring 10.*

5 Summary

In 2004 the Swedish Nuclear Fuel and Waste Management Co. (SKB) initiated the project "Task Force on Engineered Barrier Systems". This project has the objective to verify the feasibility of modelling THM-coupled processes (task 1) and gas migration processes (task 2) in clay-rich buffer materials. The tasks are performed on the basis of appropriate benchmarks.

This report documents the modelling results of the THM-benchmark 2.2 which is the Canister Retrieval Test (CRT) using the code GeoSys/RockFlow. The Temperature Buffer Test (TBT) which was performed in the immediate vicinity of the CRT is included in the model.

For this benchmark hydraulic processes were monitored only in the buffer, not in the rock. The artificial saturation of the buffer in both experiments via surrounding filters would have allowed for modelling the hydraulic processes in the buffer with axially symmetric models. The modelling of the artificial saturation with a pressure boundary condition (measured values) does not require detailed information on the hydraulic properties of the rock. The water inflow to the filters was also measured and – if used as source term in the model – would have required more detailed information on the hydraulic properties of the rock. Especially the heat transport requires the handling of the problem in 3-D. Due to limitations imposed by post-processing different spatial discretisations of the model had to be used during the processing of the benchmark.

The calculated temperature values for the rock and CRT generally agree well with the measured data. The model shows a tendency both to over- or underestimate the measured temperature for specific sensors, therefore an improvement of the model might not succeed without taking into account for example discontinuities in the rock. For the TBT the model clearly underestimates the measured temperatures.

Concerning hydraulic parameters the values of permeability and tortuosity (i.e. thermal vapour diffusion coefficient) were varied in the calculations. The time necessary to saturate the buffer is very sensitive to both these values. The influence of tortuosity in the calculations is more significant at lower permeabilities and for regions in the buffer close to the heater. For the CRT there is some indication that the inner gap between heater and bentonite rings was filled with water when the outer gap between bentonite and the wall of the deposition hole was filled with bentonite pellets and water. However, in the modelling results presented here the inner gap was assumed to be dry. For the calculation of TBT the saturation via the sand filter starts earlier than in reality. In general the degree of agreement between calculated and measured data differs between the sensors. Taking into account the uncertainty of the initial hydraulic state of CRT's bentonite rings at the inner gap and the general difficulties of measuring water content a real calibration of permeability and tortousity values against these in situ data is not possible. However, the overall agreement of calculated and measured values still is relatively reasonable.

This report only documents calculation results for total pressure from a first approach of discretizing the model geometry. Further calculations which were meant to check the influence of the outer bentonite layer and further mechanical parameter values unfortunately had to be discarded due to severe post-processing problems: it was not possible to check whether the input was correctly transferred into the numerical model.

Overall, the THM-benchmarks of the first phase of the project Task Force on Engineered Barrier Systems were modelled successfully with the code GeoSys/RockFlow. However, the governing equations which can be found in detail for example in WANG et al. (2009) have to be considered as simplifications with respect to hydraulic and mechanical processes. For modelling a closed and backfilled repository the necessity to model the gas phase needs to be checked. Though the description of the mechanical processes with the simple water saturation dependency succeeded especially in the laboratory benchmarks 1 (compare NOWAK 2007), the mechanical processes in a swelling bentonite buffer are much more complex. The use of the 3-D capability of the code was used beyond the intended purpose of the benchmarks as exercise to model real repository layouts in complex geological structures.

6 References

ÅKESSON, M. (2006): Temperature Buffer Test, Evaluation modeling - Field test. - Svensk Kärnbränslehantering, **IPR-06-10**: 297 p., 5 fig., 6 app.; Stockholm.

NOWAK, T. (2007): Task Force on Engineered Barrier Systems, Modelling of THM-coupled processes for Task 1, Benchmarks 1, using GeoSys/RockFlow. - Svensk Kärnbränslehantering, **IPR-07-13**: 47 p., 30 fig., 3 tab.; Stockholm.

NOWAK, T. & KUNZ, H. (2009): Task Force on Engineered Barrier Systems, Modelling of THM-coupled processes for benchmark 2.1.1 and 2.1.2 with the code GeoSys/RockFlow. - Svensk Kärnbränslehantering, **IPR-09-14**: 57 p., 46 fig., 7 tab.; Stockholm.

SHAO, H. & NOWAK, T. (2008): DECOVALEX IV - THMC Summary and Achievement. - Federal Institute for Geosciences and Natural Resources, **10075/08**: 148 p.; Hannover.

WANG, W., KOSAKOWSKI, G. & KOLDITZ, O. (2009): A parallel finite element scheme for thermo-hydro-mechanical coupled problems in porous media. Computers & Geosciences 35, 1631-1641.